Comparison of Detection Templates for Gravitational Waves from Inspiralling Compact Binaries

Bala Iyer

Raman Research Institute
Bangalore India

IHP
2006

Introduction

- Late Inspiral and Merger Epochs of ICB (NS or BH) are the most important sources for LI GW Detectors like LIGO and VIRGO.
- The waveform is a chirp
  Amplitude and Frequency increasing with Time
- GW are WEAK SIGNALS buried in NOISE of detector
- Require Matched Filtering (MF) Both for their Detection or Extraction and Parameter Estimation
- Success of MF requires
  Accurate model of signal using Gen Rel;
- Favours sources like ICB (NS-NS, BH-BH, NS-BH)

Chirp, Matched Filtering

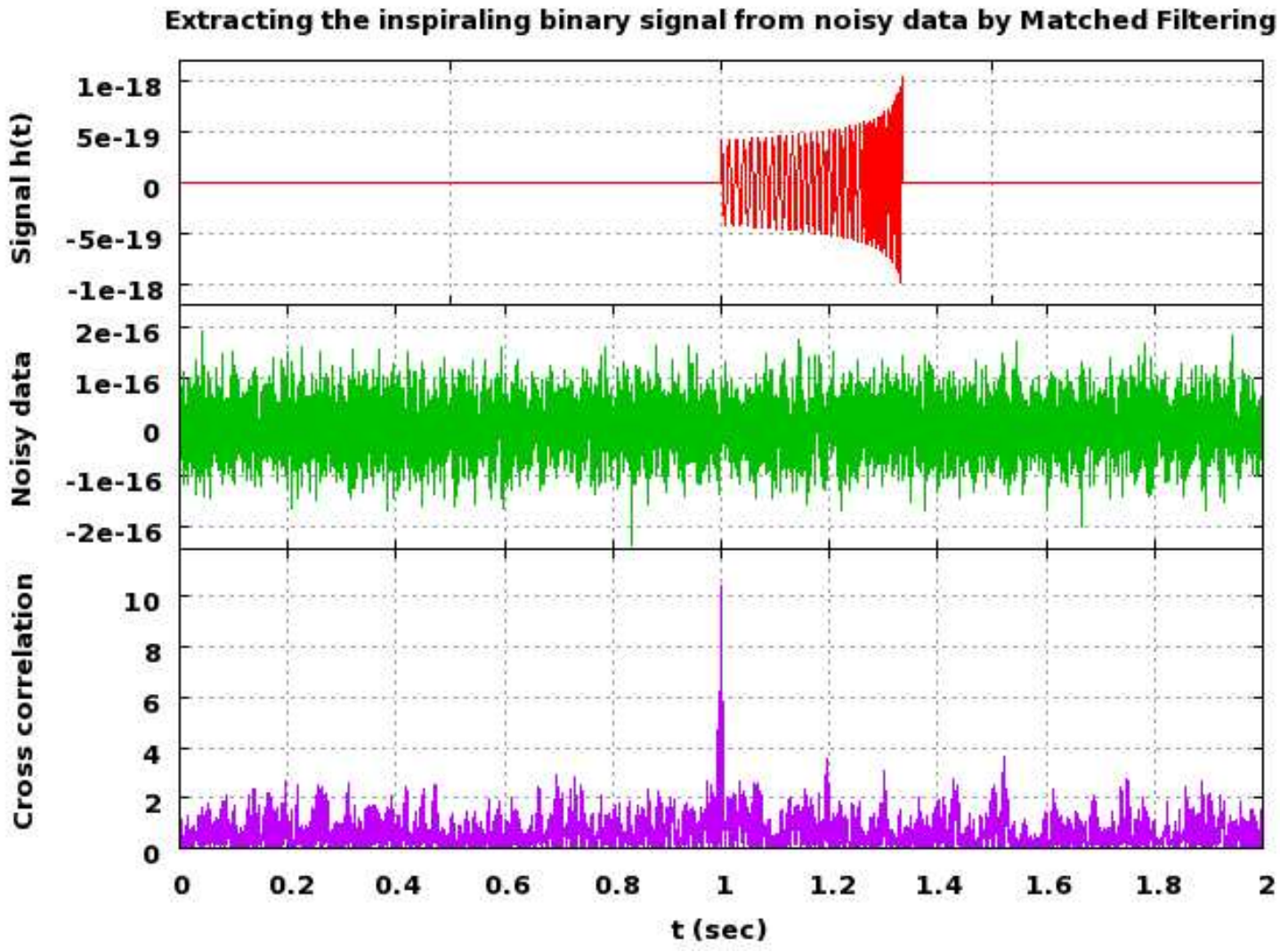

From Anand Sengupta (IUCAA)

Stages of Binary Coalescence

- Inspiral: well modelled by PN Approx methods in the general two body case (3.5PN) and Pertbn Methods in the test body approximation (5.5PN)
- nPN means corrections of order $(v^2/c^2)^n$ relative to leading order
- Late Inspiral, Plunge: Extended approximation methods like EOB (2PN/3PN)
- Merger: Fully GR Soln of EE - Numerical Relativity
- QNM Ringdown: BH Pertbn Theory
- This Study is restricted to inspiral phase

Standard Approach to Phasing

- Grav Radn Reaction reduces eccentricity so that ICB move in (quasi) circular orbits in the late epochs
- Work in the Adiabatic Approximation:

$$\dot{\omega}_{\rm orb}/\omega^2_{\rm orb} \ll 1$$

Change in Orbital Frequency small compared to Orbital frequency; Adiabatic Inspiral

- Circular orbit may be characterised by a PN conserved Energy
- Inspiral characterised by the associated PN GW Luminosity

Standard ... Contd

- GW Phasing follows from the Balance Eqn

$$\dot{E}(v) = -\mathcal{F}(v)$$

$$v = \left(\frac{Gm\omega_{\rm orb}}{c^3}\right)^{1/3}$$

- GW polarisations

$$h_{+,\times} = \frac{2G\mu}{c^2 R}\ v^2\ \times\{H^{(0)}_{+,\times} + vH^{(1/2)}_{+,\times} + \cdots + v^5 H^{(5/2)}_{+,\times}\}$$

$$H^{(0)}_{+} = -(1+c_i^2)\cos 2\phi,$$

$$H^{(0)}_{\times} = -2c_i \sin 2\phi, \cdots$$

Newtonian Phasing Formula

- Use E, the CM energy at Newtonian order and $\mathcal{L}$, GW luminosity or energy flux

$$E = -\frac{1}{2}\mu c^2 x$$

$$\mathcal{L} = \frac{32}{5}\ \frac{c^5}{G}\ \nu^2 x^5$$

$$\frac{c^5}{G} \approx 3.63 \times 10^{52}\ \mathrm{W},$$

- and heuristic Energy Balance equation

$$\frac{dE}{dt} = -\mathcal{L}.$$

N Phasing ...Contd..

$$x(t) = \frac{1}{4}\tau^{-1/4}$$

$$\tau = \frac{c^3\nu}{5Gm}(t_c - t)$$

$$\phi = \int \omega dt = -\frac{5}{\nu}\int x^{2/3} d\tau$$

- Number of GW cycles $\mathcal{N}$ left until coalescence starting at some frequency ω

$$\mathcal{N} = \frac{\phi_c - \phi}{\pi} = \frac{1}{32\pi\nu}x^{-5/2}$$

- $\propto (v/c)^{-5}$ (inverse of $(v/c)^5$ the RR order)

N Phasing ... Contd

- ~ 16000 cycles for NS-NS binaries

- Matched filtering requires accuracy to about fraction of a cycle.

- Formally (and detailed DA), indicate that one needs to go to relative order 2.5PN or 3PN in $\mathcal{L}$ to achieve the required accuracy.
  (Damour, BRI, Sathyaprakash - 1998, 2000, 2001, 2002)
  (Damour, BRI, Jaranowski, Sathyaprakash - 2003)
  (Buonanno, Chen, Vallisneri - 2003)

Current Status

- Templates in Test Mass Limit: 5.5PN
  Tanaka, Tagoshi, Sasaki (1996)
- Templates: Phase - 3.5PN (2004)
  Blanchet, G. Faye, BRI, Joguet (2002)
  Blanchet, Damour, Esposito-Farese, BRI (2004)
- Templates: Amplitude - 2.5PN (2004)
  K. Arun, L. Blanchet, BRI and Moh'd S.S. Qusailah
- Restricted Wave Approximation: Phase at best PN accuracy; Amplitude Newtonian; Dominant Harmonic at Twice Orbital Frequency

$$h(t) = \frac{4A\eta m}{D} v^2(t) \cos[\varphi(t) + \varphi_C],$$

- Full Waveform - Fourier Domain -SPA
  2.5 PN Amplitude, 3.5 PN Phase
  Van Den Broeck and Sengupta 05, 06

PART I

Comparison of Search Templates for GW from Binary Inspiral

Based on

T. Damour, B.R. Iyer and B S Sathyaprakash

Phys. Rev. D **63**, 044023 (2001)

GWDA Problem

- In searching for GW from ICB one is faced with the following data analysis problem: We have some (unknown) exact GWF $h^X(t;\lambda_k)$ where λ_k, $k=1,\ldots,n_\lambda$, are the parameters of the signal (e.g., masses m_1 and m_2). We have theoretical calculations of the motion and gravitational radiation from binary systems consisting of (NS) or (BH) giving the PN expansions of an energy function $E(x\equiv v^2)$, which is related to the total relativistic energy $E_{\rm tot}$ via $E_{\rm tot}=(m_1+m_2)(1+E)$, and a GW luminosity (or "flux") function $\mathcal{F}(v)$. The dimensionless argument $v\equiv x^{\frac{1}{2}}$ is an invariantly defined "velocity" related to the instantaneous GW frequency F (= twice the *orbital* frequency) by $v\equiv(\pi mF)^{\frac{1}{3}}$.
- Given PN expansions of the motion of and grav radn from a binary system, one needs to compute the *"phasing formula"*, i.e. an accurate mathematical model for the evolution of the GW phase (within the "restricted" waveform approximation which keeps only the leading harmonic in the GW signal) $\phi^{\rm GW}=p[t;\lambda_i]$, involving the set of parameters $\{\lambda_i\}$ carrying information about the emitting binary system.

Phasing formula - Adiabatic Approx

- In the adiabatic approximation the phasing formula is easily derived from the energy and flux functions. Standard energy-balance equation $dE_{\rm tot}/dt = -\mathcal{F}$ gives the following parametric representation of the phasing formula:

$$t(v) = t_{\rm ref} + m \int_v^{v_{\rm ref}} dv\, \frac{E'(v)}{\mathcal{F}(v)}, \quad \phi(v) = \phi_{\rm ref} + 2 \int_v^{v_{\rm ref}} dv v^3\, \frac{E'(v)}{\mathcal{F}(v)},$$

  $t_{\rm ref}$ and $\phi_{\rm ref}$ are integration constants and $v_{\rm ref}$ an arbitrary reference velocity.

- From the view point of computation more efficient to work with the following pair of coupled, non-linear, ordinary differential equations (ODE's) that are equivalent to the above parametric formulas:

$$\frac{d\phi}{dt} - \frac{2v^3}{m} = 0, \quad \frac{dv}{dt} + \frac{\mathcal{F}(v)}{mE'(v)} = 0.$$

- For massive systems, adiabatic approximation fails and one must replace the two ODE's by a more complicated ODE system.

T-approximants

- Denote by E_{T_n} and $\mathcal{F}_{T_n}$ the $n^{\rm th}$-order. "Taylor" approximants (as defined by the PN expansion) of the energy and flux functions. (Label n refers to an approximant accurate up toa $v^n = x^{(n/2)}$ included)

$$E_{T_{2n}}(x) \equiv E_N(x) \sum_{k=0}^{n} \hat{E}_k(\eta) x^k,$$

$$\mathcal{F}_{T_n}(x) \equiv \mathcal{F}_N(x) \left[\sum_{k=0}^{n} \hat{\mathcal{F}}_k(\eta) v^k + \sum_{k=6}^{n} \hat{L}_k(\eta) \log(v/v_0) v^k \right],$$

$$\text{where, } E_N(x) = -\frac{1}{2}\eta x, \quad \mathcal{F}_N(x) = \frac{32}{5}\eta^2 x^5.$$

Subscript N denotes the "Newtonian value", $\eta \equiv m_1 m_2/m^2$ the symmetric mass ratio, and v_0 is a fiducial constant to be chosen below.

T-approximants

- In the test mass limit, i.e. $\eta \to 0$, $E(x)$ is known exactly, from which the Taylor expansion of $E_{T_n}(v,0)$, can be computed to all orders. In the $\eta \to 0$ limit, the exact flux is known numerically and the Taylor expansion of flux is known up to order $n = 11$
(Poisson 93, Tanaka et al 96).
- For η finite, the above Taylor approximants are known up to seven-halves PN order, i.e. $n = 7$. (Damour, Jaranowski, Schäfer; Blanchet, Faye, Iyer, Joguet; Blanchet, Damour, Esposito-Farese, Iyer)
- Problem is to construct a sequence of approximate waveforms $h^A_n(t;\lambda_k)$, starting from the PN expansions of $E(v)$ and $\mathcal{F}(v)$. In formal terms, any such construction defines a *map* say T from the set of the Taylor coefficients of E and $\mathcal{F}$ into the (functional) space of waveforms

$$(E_{T_n}\ ,\ \mathcal{F}_{T_n}) \stackrel{T}{\to} h^T_n(t,\lambda_k)\ ,$$

obtained by inserting the successive Taylor approximants into the phasing formula. For brevity, refer to these "Taylor" approximants as " T-approximants".

T-approximants

- Beware: Even within this Taylor family of templates, there are at least three ways of proceeding further, leading to the following three *inequivalent* constructs:

Taylor $T1$ Approximant

- To compute $v(t)$ and $\phi(t)$;
  Std approach to Evoln of the GWF under RR:
  Adiabatic approximation;
  Cutler et al (1993)
- E and $\mathcal{F}$ given as PN Expansions in v
  Use E and $\mathcal{F}$ both to same *relative* PN order
- Phasing of GW given by following coupled ODE

$$\frac{d\varphi}{dt} = \frac{2v^3}{m}, \qquad \frac{dv}{dt} = -\frac{\mathcal{F}(v)}{mE'(v)},$$

  $E'(v) = dE(v)/dv$; $m = m_1 + m_2$

- Retain the rational polynomial $\mathcal{F}_{T_n}/E_{T_n}$ as it appears above
- Integrate the two ODE's numerically.
- Denote the phasing formula so obtained as $\phi^{(1)}_{T_n}(t)$:

Taylor $T2$-approximants

- Re-expand the rational function $\mathcal{F}_{T_n}/E_{T_n}$ appearing in the phasing formula and truncate it at order v^n,
- The integrals can be worked out analytically, to obtain a *parametric* representation of the phasing formula in terms of polynomial expressions in the auxiliary variable v

$$\phi^{(2)}_{T_n}(v) = \phi^{(2)}_{\rm ref} + \phi^v_N(v)\sum_{k=0}^{n}\hat{\phi}^v_k v^k, \quad t^{(2)}_{T_n}(v) = t^{(2)}_{\rm ref} + t^v_N(v)\sum_{k=0}^{n}\hat{t}^v_k v^k,$$

- The superscript on the coefficients (eg. ϕ^v_1) indicates that v is the expansion parameter
- The coefficient of ϕ^v_k include in some cases, a $\log v$ dependence

Taylor $T3$-approximants

- Alternatively, the second of the polynomials in Eq. (t as fn of v) can be inverted to obtain a polynomial for v in terms of t
- This can be substituted in $\phi^{(2)}(v)$ to arrive at an explicit time-domain phasing formula

$$\phi^{(3)}_{T_n}(t) = \phi^{(3)}_{\rm ref} + \phi^t_N \sum_{k=0}^{n} \hat{\phi}^t_k \theta^k, \qquad F^{(3)}_{T_n}(t) = F^t_N \sum_{k=0}^{n} \hat{F}^t_k \theta^k,$$

$\theta = [\eta(t_{\rm ref} - t)/(5m)]^{-1/8}$ and $F \equiv d\phi/2\pi dt = v^3/(\pi m)$ is the instantaneous GW frequency.

- The coefficients in these expansions are all listed in DIS

Padé Re-Summation

- Padé re-summation, is a standard mathematical technique used to accelerate the convergence of poorly converging power series.
- Let $S_n(v) = a_0 + a_1\, v + \cdots + a_n\, v^n$ be a truncated Taylor series. A Padé approximant of the function whose Taylor approximant to order v^n is S_n is defined by two integers m, k such that $m + k = n$. If $T_n[\cdots]$ denotes the operation of expanding a function in Taylor series and truncating itto accuracy v^n (included), the P_k^m Padé approximant of S_n is defined by

$$P_k^m(v) = \frac{N_m(v)}{D_k(v)};\;\; T_n[P_m^k(v)] \equiv S_n(v),$$

N_m and D_k are *polynomials* in v of order m and k respectively. If one assumes that $D_k(v)$ is normalised so that $D_k(0) = 1$; i.e. $D_k(v) = 1 + q_1\, v + \cdots$, one shows that Padé approximants are uniquely defined by Eq. above. Most useful Padé approximants are the ones near the "diagonal", $m = k$, i.e. P_m^m if $n = 2m$ is even, and P_m^{m+1} or P_{m+1}^m if $n = 2m + 1$ is odd.

Padé Re-Summation

- We shall use the diagonal (P^m_m) and the "sub-diagonal" (P^m_{m+1}) approximants which can be conveniently written in a continued fraction form. For example, given $S_2(v) = a_0 + a_1\, v + a_2\, v^2$ one looks for

$$P^1_1(v) = \frac{c_0}{1 + \frac{c_1 v}{1+c_2 v}} = \frac{c_0(1+c_2 v)}{1+(c_1+c_2)v}.$$

- A convenience of this form is that the n-th continued-fraction coefficient c_n depends only on the knowledge of the PN coefficients of order $\leq n$.

- The continued fraction Padé coefficients of a series containing six terms, i.e. $S_5(v)$, are given by

$$\begin{aligned}
c_0 &= a_0, \quad c_1 = -\frac{a_1}{a_0}, \quad c_2 = -\frac{a_2}{a_1} + \frac{a_1}{a_0}, \quad c_3 = \frac{a_0(a_1 a_3 - a_2^2)}{a_1(a_1^2 - a_2 a_0)} \\
c_4 &= -\frac{c_0 c_1 (c_2+c_1)^3 + c_0 c_1 c_2 c_3 (c_3 + 2c_2 + 2c_1) - a_4}{c_0 c_1 c_2 c_3}, \\
c_5 &= -\frac{((c_2+c_1)^2 + c_2 c_3)^2}{c_2 c_3 c_4} - \frac{(c_4+c_3+c_2+c_1)^2}{c_4} - \frac{a_5}{c_0 c_1 c_2 c_3 c_4}.
\end{aligned}$$

P - Approximants

- Proposal: Re-sum the Taylor expansions (in powers of v) of the energy and flux functions.
- Starting from the PN expansions of E and $\mathcal{F}$, construct a new class of waveforms, called *P-approximants*, based on two essential ingredients:
- (i) the introduction, on theoretical grounds, of two new, supposedly more basic and hopefully better behaved, energy-type and flux-type functions, say $e(v)$ and $f(v)$, and
- (ii) the systematic use of Padé approximants (instead of straightforward Taylor expansions) when constructing successive approximants of the intermediate functions $e(v)$, $f(v)$. Schematically, our procedure is based on the following map, say "P":

$$(E_{T_n}, \mathcal{F}_{T_n}) \to (e_{T_n}, f_{T_n}) \to (e_{P_n}, f_{P_n}) \to (E[e_{P_n}], \mathcal{F}[e_{P_n}, f_{P_n}]) \to h_n^P(t, \lambda_k).$$

P - Approximants

- The new energy function $e(x)$, where $x \equiv v^2$, is constructed out of the total relativistic energy $E_{\rm tot}(x)$ using

$$e(x) \equiv \left(\frac{E_{\rm tot}^2 - m_1^2 - m_2^2}{2m_1 m_2} \right)^2 - 1.$$

- Function $E(x)$ entering the phasing formulas is the total energy per unit mass after subtracting out the rest mass energy: $E(x) = [E_{\rm tot}(x) - m]/m$ and is given in terms of $e(x)$ by

$$E(x) = \left[1 + 2\eta \left(\sqrt{1+e(x)} - 1 \right) \right]^{1/2} - 1, \quad \frac{dE}{dx} = \frac{\eta e'(x)}{2\left[1+E(x)\right]\sqrt{1+e(x)}}.$$

Note that the quantity $E'(v)$, needed in the phasing formula, is related to $dE(x)/dx$ via $E'(v) = 2v dE(x)/dx$. In the test-mass limit $e(x)$ and $dE(x)/dx$ are known exactly:

$$e_{\eta=0}(x) = -x\frac{1-4x}{1-3x}, \quad E^{\eta=0}(x) = \eta \left(\frac{1-2x}{\sqrt{1-3x}} - 1 \right), \quad \frac{dE^{\eta=0}}{dx} = -\frac{\eta}{2}\frac{(1-6x)}{(1-3x)^{3/2}}$$

P - Approximants

- The rationale for using $e(x)$ as the basic quantity rather than $E_{\rm tot}(x)$ are the following two points:
- (1) In the test mass case $e(x)$ is meromorphic in the complex x-plane, with a simple pole singularity, while the function $E(x)$ is non-meromorphic and exhibits a branch cut.
- (2) Secondly, in the test mass case, the Padé approximant of $e_{T_{2n}}(x)$, for $n \geq 2$, yields the known exact expression including the location of the Iso and the pole. Therefore, the function $e(x)$ is more suitable in analyzing the analytic structure than is $E(x)$.
- In the comparable mass case, under the assumption of structural stability between the case $\eta \to 0$ and the case of finite η, one can expect the exact function $e(x)$ to admit a simple pole singularity on the real axis $\propto (x - x_{\rm pole})^{-1}$. We do not know the location of this singularity, but Padé approximants are excellent tools for giving accurate representations of functions having such pole singularities.

P - Approximants

- Proposal: Given some usual Taylor approximant to the normal energy function, $E_{T_{2n}} = -\frac{1}{2}\,\eta\,x\,(1 + E_1\,x + E_2\,x^2 + \cdots + E_n\,x^n)$, one first computes the corresponding Taylor approximant for the e function, say

$$e_{T_{2n}}(x) = -x \sum_{k=0}^{n} e_k x^k.$$

Then, one defines the Padé approximant of $e_{T_{2n}}(x)$ More precisely, $e_{P_{2n}}(x)$ is $-x$ times the Padé approximant of $-x^{-1}e_{T_{2n}}(x)$.)

$$e_{P_{2n}}(x) \equiv -x\,P^m_{m+\epsilon}\left[\sum_{k=0}^{n} e_k\,x^k\right]$$

$\epsilon = 0$ or 1 depending on whether $n \equiv 2m + \epsilon$ is even or odd. We shall call the continued fraction Padé coefficients of $e_{P_{2n}}$ as $c_1, c_2, \cdots,$ (Note that $c_0 \equiv 1$). They are given in terms of e_k.

P - Approximants

- Given a continued fraction approximant $e_{P_{2n}}(x)$ of the truncated Taylor series $e_{T_{2n}}$ of the energy function $e(x)$ the corresponding $E_{P_{2n}}(x)$ and $dE_{P_{2n}}(x)/dx$ functions are obtained using earlier formulas by replacing $e(x)$ on the right hand side with $e_{P_{2n}}(x)$.
- Apart from using it to improve the convergence of the PN series, it is proposed to use the Padé-resummed function $e_{P_{2n}}(x)$ to determine the location of the lso, the Padé estimates of the lso being defined by considering the minima of $e_{P_{2n}}(x)$. In contrast, in the Taylor case one must, for consistency, use the minima of $E_{T_n}(v)$ to define the locations of the lso.
- One can check that in the test mass case this Padé-based method yields the exact result at orders v^4 and beyond while the corresponding Taylor-based method (considering the minima of $E_{T_n}(v)$) gives unacceptably high estimates of $v_{\rm lso}$, i.e. of the GW frequency at the lso . In the finite η case, the Padé-resummed predictions are in good qualitative, (and reasonable quantitative) agreement with the more recent predictions based on the "effective-one-body" approach.

P - Approximants

- Having defined a new energy function, introduce a new flux function. The aim is to define an analytic continuation of the flux function to control its analytic structure as also to handle the logarithmic terms that appear in the flux function. Factoring out the logarithmic terms is what allows us to use standard Padé techniques effectively in this problem.
- It has been pointed out that the flux function in the test mass case $\mathcal{F}(v;\eta=0)$ has a simple pole at the light ring $v^2=1/3$. It has been argued that the origin of this pole is quite general and that even in the case of comparable masses we should expect to have a pole singularity in $\mathcal{F}$. However, as already pointed out, the light ring orbit in the $\eta\neq 0$ case corresponds to a simple pole $x_{\rm pole}(\eta)$ in the new energy function $e(x;\eta)$. Let us define the corresponding (invariant) "velocity" $v_{\rm pole}(\eta)\equiv\sqrt{x_{\rm pole}(\eta)}$. This motivates the introduction of the following "factored" flux function, $\hat{f}(v;\eta)$

$$\hat{f}(v;\eta)\equiv(1-v/v_{\rm pole})\;\hat{\mathcal{F}}(v;\eta).$$

$\hat{\mathcal{F}}(v)\equiv\mathcal{F}(v)/\mathcal{F}_N(v)=5\mathcal{F}(v)/(32\eta^2v^{10})$, is the Newton-normalised flux.

P - Approximants

- Multiplying by $1 - v/v_{\rm pole}$ rather than $1 - (v/v_{\rm pole})^2$ has the advantage of regularizing the structure of the Taylor series of $\hat{f}(v)$ introducing a term linear in v, which is absent in the flux function.
- Three further inputs will allow us to construct better converging approximants to $\hat{f}(v)$.
- First, it is clear (if we think of v as having the dimension of a velocity) that one should normalize the velocity v entering the logarithms in the flux function to some relevant velocity scale v_0. In the absence of further information the choice $v_0 = v_{\rm lso}(\eta)$ seems justified (the other basic choice $v_0 = v_{\rm pole}$ is numerically less desirable as v will never exceed $v_{\rm lso}$ and we wish to minimize the effect of the logarithmic terms).
- A second idea, to reduce the problem to a series amenable to Padéing, is to factorize the logarithms. This is accomplished by writing the $\hat{f}$ function in the form

P - Approximants

$$\hat{f}_{T_n}(v;\eta) = \left(1 + \sum_{k=6}^{n} \hat{l}_k v^k \ln \frac{v}{v_{\rm lso}}\right)\left(\sum_{k=0}^{n} \hat{f}_k v^k\right),$$

Coefficients $\hat{f}_k$ are $\hat{f}_0 = 1$, $\hat{f}_{k+1} = \hat{\mathcal{F}}_{k+1} - \hat{\mathcal{F}}_k/v^{\rm pole}$ and $\hat{l}_k$ are constants determined from the coefficients of $\hat{\mathcal{F}}_k$. Variables are 'hatted' here as a reminder that they represent coefficients of Newtonian-normalised quantities.

- Finally, we define Padé approximants to the factored flux function $\hat{f}(v)$ as

$$\hat{f}_{P_n}(v;\eta) \equiv \left(1 + \sum_{k=6}^{n} \hat{l}_k v^k \ln \frac{v}{v_{\rm lso}^{P_n}(\eta)}\right) P^m_{m+\epsilon}\left(\sum_{k=0}^{n} \hat{f}_k v^k\right),$$

$v_{\rm lso}^{P_n}(\eta)$ denotes the lso velocity ($\equiv \sqrt{x_{\rm lso}}$) for the v^n-accurate Padé approximant of $e(x)$, and where $P^m_{m+\epsilon}$ denotes as before a diagonal or sub-diagonal Padé with $n \equiv 2m + \epsilon$, $\epsilon = 0$ or 1.

P - Approximants

- The corresponding approximant of the flux $\hat{\mathcal{F}}(v)$ is then defined as

$$\hat{\mathcal{F}}_{P_n}(v;\eta) \equiv \left(1 - \frac{v}{v_{\rm pole}^{P_n}(\eta)}\right)^{-1} \hat{f}_{P_n}(v;\eta),$$

$v_{\rm pole}^{P_n}(\eta)$ denotes the pole velocity defined by the v^n-Padé of $e(x)$. In the test mass case the exact location of the pole and the lso are $x_{\rm pole} = 1/3$ and $x_{\rm lso} = 1/6$, respectively. We shall denote the continued fraction Padé coefficients of $\hat{f}_{P_n}(v)$ by d_k.

Frequency-domain phasing- Adiabatic Approx

- Frequency-domain phasing uses the usual stationary phase approximation for chirp signals. Consider a signal of the form,

$$h(t) = 2a(t)\cos\phi(t) = a(t)\left[e^{-i\phi(t)} + e^{i\phi(t)}\right],$$

  $\phi(t)$ is the implicit solution of one of the phasing formulas in the phasing eqn for some choice of functions E' and $\mathcal{F}$.

- Quantity $2\pi F(t) = d\phi(t)/dt$ defines the instantaneous GW frequency $F(t)$, and is assumed to be continuously increasing. (We assume $F(t) > 0$.) Fourier transform $\tilde{h}(f)$ of $h(t)$ is defined as

$$\tilde{h}(f) \equiv \int_{-\infty}^{\infty} dt e^{2\pi i f t} h(t) = \int_{-\infty}^{\infty} dt\, a(t)\left[e^{2\pi i f t - \phi(t)} + e^{2\pi i f t + \phi(t)}\right].$$

  Above transform can be computed in the SPA. For positive frequencies only the first term on the right contributes and yields the following *usual* SPA:

$$\tilde{h}^{\rm uspa}(f) = \frac{a(t_f)}{\sqrt{\dot{F}(t_f)}} e^{i\left[\psi_f(t_f) - \pi/4\right]}, \quad \psi_f(t) \equiv 2\pi f t - \phi(t),$$

Frequency-domain phasing- Adiabatic Approx

- t_f is the saddle point defined by solving for t, $d\psi_f(t)/dt = 0$, i.e. the time t_f when the GW frequency $F(t)$ becomes equal to the Fourier variable f. In the (adiabatic) approximation, the value of t_f is given by the following integral:

$$t_f = t_{\rm ref} + m \int_{v_f}^{v_{\rm ref}} \frac{E'(v)}{\mathcal{F}(v)} dv,$$

  $v_f \equiv (\pi m f)^{1/3}$. Using t_f from the above equation and $\phi(t_f)$ one finds that

$$\psi_f(t_f) = 2\pi f t_{\rm ref} - \phi_{\rm ref} + 2 \int_{v_f}^{v_{\rm ref}} (v_f^3 - v^3) \frac{E'(v)}{\mathcal{F}(v)} dv.$$

- Big computational (with respect to its time-domain counterpart) advantage, is that, in the frequency domain, there are no equations to solve iteratively; the Fourier amplitudes are given as explicit functions of frequency.
- In the Fourier domain too there are many inequivalent ways in which the phasing ψ_f can be worked out. The most popular being

$F1$ - Approximant

- Substitute (without doing any re-expansion or re-summation) for the energy and flux functions their PN expansions or the P-approximants of energy and flux functions and solve the integral in Eq. numerically to obtain the T-approximant SPA or P-approximant SPA, respectively.

F2 - Approximant

- Use PN expansions of energy and flux but re-expand the ratio $E'(v)/\mathcal{F}(v)$ in Eq. in which case the integral can be solved explicitly. This leads to the following explicit, Taylor-like, Fourier domain phasing formula:

$$\psi_f(t_f) = 2\pi f t_{\rm ref} - \phi_{\rm ref} + \tau_N \sum_{k=0}^{5} \hat{\tau}_k (\pi m f)^{(k-5)/3}$$

  $\hat{\tau}_k$ are the chirp parameters listed in the paper. The latter is one of the standardly used frequency-domain phasing formulas. Therefore, one uses that as one of the models in our comparison of different inspiral model waveforms. Refer to it as "type-f2" frequency-domain phasing.

- Just as in the time-domain, the frequency-domain phasing is most efficiently computed by a pair of coupled, non-linear, ODE's:

$$\frac{d\psi}{df} - 2\pi t = 0, \quad \frac{dt}{df} + \frac{\pi m^2}{3v^2}\frac{E'(f)}{\mathcal{F}(f)} = 0,$$

  rather than by numerically computing the integral in Eqs.

Edge corrections...

- One can correct the performance of the usual SPA by including *edge corrections* arising as a consequence of modeling the time-domain signal as being abruptly terminated at a time $t = t_{\rm max}$ (*time-truncated chirp*) when the GW frequency reaches $F = F_{\rm max}$. In practice, we expect that $F_{\rm max}$ will be of order the GW frequency at the Iso. However, we prefer to leave unspecified the exact value of $F_{\rm max}$. The idea is to use $F_{\rm max}$ as a free model parameter, to be varied so as to maximize the overlap between the $t_{\rm max}$-truncated template and the real signal. Such time-truncated signals can be represented as:

$$h(t) = 2a(t)\cos\phi(t)\theta(t_{\rm max} - t),$$

  θ denotes the Heaviside step function, i.e. $\theta(x) = 0$ if $x < 0$ and $\theta(x) = 1$ when $x \geq 0$.

- Effect of this time-windowing has been modeled in DIS2 and the result is that the Fourier transform of such a time-truncated signal can be accurately represented in the two regions $f \leq F_{\rm max}$ and $f \geq F_{\rm max}$, by using complementary error function *erfc*

Time-domain - Beyond Adiabatic Approx

- In the standard "adiabatic approximation", one estimates the phasing by combining the energy-balance equation $dE_{\rm tot}/dt = -\mathcal{F}$ with some Taylor or resummed estimates for the energy and flux as functions of the instantaneous circular orbital frequency.
- Buonnano and Damour, 2000 introduced a new approach to GW from coalescing binaries which is no longer limited to the adiabatic approximation, and which is expected to describe rather accurately the transition between the inspiral and the plunge, and to give also a first estimate of the following plunge signal.
- The approach is essentially a re-summation technique which consists of two main ingredients:
- (i) the "conservative" (damping-free) part of the dynamics (effectively equivalent to the specification of the $E(v)$ in the previous approaches) is resummed by a new technique which replaces the two-body dynamics by an effective one-body dynamics and

Time-domain - Beyond Adiabatic Approx

- (ii) the "damping" part of the dynamics (equivalent to the specification of the $\mathcal{F}(v)$) is constructed by the re-summation technique discussed earlier.
- Time-domain waveform is obtained as the following function of the reduced time $\hat{t} = t/m$:

$$h(\hat{t}) = \mathcal{C}\, v_\omega^2(\hat{t}) \cos(\phi_{\rm GW}(\hat{t}))\,, \quad v_\omega \equiv \left(\frac{d\varphi}{d\hat{t}}\right)^{\frac{1}{3}}\,, \quad \phi_{\rm GW} \equiv 2\varphi\,.$$

Orbital phase $\varphi(\hat{t})$ entering Eq. is given by integrating a system of ODE's:

$$\begin{aligned}
\frac{dr}{d\hat{t}} &= \frac{\partial \widehat{H}}{\partial p_r}(r, p_r, p_\varphi)\,,\\
\frac{d\varphi}{d\hat{t}} &= \widehat{\omega} \equiv \frac{\partial \widehat{H}}{\partial p_\varphi}(r, p_r, p_\varphi)\,,\\
\frac{dp_r}{d\hat{t}} &+ \frac{\partial \widehat{H}}{\partial r}(r, p_r, p_\varphi) = 0\,,\\
\frac{dp_\varphi}{d\hat{t}} &= \widehat{\mathcal{F}}_\varphi(\widehat{\omega}(r, p_r, p_\varphi))\,.
\end{aligned}$$

Time-domain - Beyond Adiabatic Approx

- Reduced Hamiltonian $\widehat{H}$ (of the associated one-body problem) is given, at the 2PN approximation, by

$$\widehat{H}(r,p_r,p_\varphi) = \frac{1}{\eta}\sqrt{1+2\eta\left[\sqrt{A(r)\left(1+\frac{p_r^2}{B(r)}+\frac{p_\varphi^2}{r^2}\right)}-1\right]},$$

$$\text{where}\quad A(r)\equiv 1-\frac{2}{r}+\frac{2\eta}{r^3}\,,\qquad B(r)\equiv\frac{1}{A(r)}\left(1-\frac{6\eta}{r^2}\right).$$

  3PN version of $\widehat{H}$ is also available in Damour, Jaranowski and Schäfer and its DA implication in Damour, Iyer, Jaranowski, Sathyaprakask

- Damping force $\mathcal{F}_\varphi$ is approximated by

$$\widehat{\mathcal{F}}_\varphi = -\frac{1}{\eta v_\omega^3}\mathcal{F}_{P_n}(v_\omega)\,,$$

  $\mathcal{F}_{P_n}(v_\omega) = \frac{32}{5}\,\eta^2\,v_\omega^{10}\,\hat{\mathcal{F}}_{P_n}(v_\omega)$ is the flux function used in P-approximants.

Time-domain - Beyond Adiabatic Approx

- System allows one to describe the smooth transition which takes place between the inspiral and the plunge. When the system becomes spuriously singular at the lso, where $E'(v_{\rm lso}) = 0$ Buonnano Damour advocated to continue using Eqs. after the transition, to describe the waveform emitted during the plunge and to match around the "light ring" to a "merger" waveform, described, in the first approximation, by the ringing of the least-damped quasi-normal mode of a Kerr black hole.
- Technique is the most complete which is available at present. It includes (in the best available approximation and for non-spinning black holes) most of the correct physics of the problem, and leads to a specific prediction for the complete waveform (inspiral + plunge + merger) emitted by coalescing binaries. Because of its completeness, we use it as our "fiducial exact" waveform in our comparison between different search templates.
- Initial data needed in computing this effective one-body waveform are as follows:

Time-domain - Beyond Adiabatic Approx

- In GWDA we are normally given an initial frequency f_0 ($\hat{\omega}_0 \equiv \pi m f_0$) corresponding to the lower cutoff of a detector's sensitivity window, at which to begin the waveform. The initial phase of the signal will not be known in advance but in order to gauge the optimal performance of our approximate templates we maximise the overlap over the initial phases of both the fiducial exact signal (EOB WF) and the approximate template. In the terminology of DIS, these fully *phase-maximised* overlaps are called the *best* overlaps.
- There are two distinct measures of the closeness of two signals: the *best* overlap (maximised over phases of both the template and the exact signal), and the *minimax* overlap (maximised over the template phase, with the worst possible exact phase).
- In this investigation (where we are interested in the optimal mathematical closeness between different signals), the *best* overlap is the mathematically cleanest measure of closeness of two families of templates In addition, we shall also maximise over the other template parameters (in particular, the masses) to get an intrinsic measure of the closeness of two families of templates.

Time-domain - Beyond Adiabatic Approx

- Note that the resulting *fully maximised* overlaps are different from the *maximised ambiguity function* of Sathyaprakash and Dhurandhar and the *fitting factor* of Apostolatos. The latter (identical, but given different names by different authors) quantities are well-defined measures of the closeness of two signals *only* within the (simplifying) approximation where signals in quadrature are orthogonal. This is, however, not the case for the signals we consider, and at the accuracy at which we are working.
- For the computation of the best overlaps, it is sufficient to construct two signal waveforms, and two template waveforms, one with phase equal to 0 and another with phase equal to $\pi/2$.

Time-domain - Beyond Adiabatic Approx

- Rest of the initial data $(r_0, p_r^0, p_\varphi^0)$ are found using

$$r_0^3 \left[\frac{1+2\eta(\sqrt{z(r_0)}-1)}{1-3\eta/r_0^2}\right] - \hat{\omega}_0^{-2} = 0, \;\; p_\varphi^0 = \left[\frac{r_0^2-3\eta}{r_0^3-3r_0^2+5\eta}\right]^{1/2} r_0,$$

$$p_r^0 = \frac{\mathcal{F}_\varphi(\hat{\omega})}{C(r_0, p_\varphi^0)(dp_\varphi^0/dr_0)}$$

$z(r)$ and $C(r, p_\varphi)$ are given by

$$z(r) = \frac{r^3 A^2(r)}{r^3-3r^2+5\eta}, \;\; C(r, p_\varphi) = \frac{1}{\eta \widehat{H}(r, 0, p_\varphi)\sqrt{z(r)}} \frac{A^2(r)}{(1-6\eta/r^2)}.$$

Plunge waveform is terminated when the radial coordinate attains the value at the light ring $r_{\rm lr}$ given by the solution to the equation,

$$r_{\rm lr}^3 - 3r_{\rm lr}^2 + 5\eta = 0.$$

Subsequent "merger" waveform is constructed as in Buonanno and Damour 2000.

Overlaps

- An important yardstick for comparing different waveforms is the *overlap*: Given two waveforms h and g their overlap is defined as

$$\mathcal{O}(h,g) = \frac{\langle h,g\rangle}{\langle h,h\rangle^{1/2}\langle g,g\rangle^{1/2}}.$$

  Scalar product $\langle , \rangle$ is defined as

$$\langle h,g\rangle = 2\int_0^\infty \frac{df}{S_h(f)}\tilde{h}(f)\tilde{g}^*(f) + C.C.$$

  C.C. denotes complex conjugation and $S_h(f)$ is the one-sided detector noise spectral density ($S_h^{\rm one-sided} = 2S_h^{\rm two-sided}$)

Overlaps

- Overlaps greater than 96.5% indicate a *good* approximation (Only 10% Loss in Events)
- SNR when detecting an "exact" signal X by means of a bank of templates A:

$$\rho \equiv \frac{S}{N} = \frac{|\langle A, X\rangle|}{\langle A, A\rangle^{1/2}} = |\mathcal{O}(A, X)|\langle X, X\rangle^{1/2}.$$

Faithfulness

- *Faithfulness*: Overlap of $A(t)$ with $X(t)$ keeping *intrinsic* parameters like masses the same for template and signal but maximising over *extrinsic* parameters like time of arrival and initial phase
- *Faithfulness*: Measure of how good is the template waveform in both detecting a signal and measuring its parameters

Effectualness

- *Effectualness*: Overlap of $A(t)$ with $X(t)$ computed by maximising over both *extrinsic* parameters like time of arrival and initial phase and *intrinsic* parameters like masses
- *Effectualness*: How good is the template waveform *only* for detection without reference to its use in estimating parameters

Results: Damour, Iyer, Sathyaprakash 01

- Fully maximised overlaps of the fiducial exact (X) waveform (effective-one-body signal) with: (1) the standard time-domain post-Newtonian approximations of type t1 and t3 ($T^{\rm t1}$, $T^{\rm t3}$), (2) the frequency-domain usual stationary phase approximations of type 1 and 2, ($T^{\rm f1}$, $T^{\rm f2}$) and (3) the time-domain P-approximants (P) – energy function, flux function. The overlaps, which are computed using the LIGO noise curve, are maximised not only over the time-lag and the initial phases of both the fiducial exact signal and the approximate template (by using two signal and two template waveforms, with phases equal to 0 and $\pi/2$ but also over the two masses m_1 and m_2 of the approximate signal models. (The optimal masses are given below the overlaps.) The time-domain $T^{\rm t3}$-approximants are terminated when $\dot{F}=0$ and the other signals are terminated when $F(t)=f_{\rm lso}$, the lso frequency being determined consistently using $E'_A(v)=0$ where $E_A(v)$ is the corresponding approximate energy function.

Results

k	$\left\langle X, T_k^{\mathrm{t1}} \right\rangle$	$\left\langle X, T_k^{\mathrm{t3}} \right\rangle$	$\left\langle X, T_k^{\mathrm{f1}} \right\rangle$	$\left\langle X, T_k^{\mathrm{f2}} \right\rangle$	$\langle X, P_k \rangle$
			$m_1 = m_2 = 15 M_\odot$		
4	0.8881	0.9488	0.8644	0.8144	0.8928
	(15.2,14.1)	(16.3, 16.4)	(14.7, 14.9)	(16.0,16.1)	(14.7, 15.1)
5	0.8794	0.8479	0.7808	0.8602	0.8929
	(17.3, 16.4)	(17.6, 17.9)	(16.8, 16.7)	(15.2,14.4)	(15.4,14.3)
			$m_1 = m_2 = 10 M_\odot$		
4	0.9604	0.9298	0.9581	0.9109	0.9616
	(10.1,9.6)	(10.5, 10.3)	(10.0, 9.7)	(10.5, 10.6)	(10.0, 10.2)
5	0.8814	0.8490	0.8616	0.9529	0.9610
	(11.4, 10.6)	(11.4, 11.7)	(10.7, 11.0)	(10.3, 9.7)	(10.4, 9.7)

Results

k	$\left\langle X, T_k^{\mathrm{t1}} \right\rangle$	$\left\langle X, T_k^{\mathrm{t3}} \right\rangle$	$\left\langle X, T_k^{\mathrm{f1}} \right\rangle$	$\left\langle X, T_k^{\mathrm{f2}} \right\rangle$	$\langle X, P_k \rangle$
			$m_1 = 10M_\odot, m_2 = 1.4M_\odot$		
4	0.9847	0.9673	0.9835	0.9721	0.9937
	(1.27,11.1)	(0.95,16.6)	(1.27, 11.1)	(0.96, 16.4)	(1.35, 10.5)
5	0.9452	0.6811	0.9394	0.9922	0.9941
	(0.82, 20.4)	(1.11, 15.7)	(0.82, 20.4)	(1.34, 10.5)	(1.37, 10.2)
			$m_1 = m_2 = 1.4M_\odot$		
4	0.8828	0.8538	0.8830	0.8503	0.9719
	(1.40, 1.39)	(1.42, 1.39)	(1.40, 1.39)	(1.44, 1.37)	(1.47, 1.34)
5	0.8522	0.7643	0.8522	0.9994	0.9945
	(1.46, 1.35)	(1.43, 1.38)	(1.46, 1.35)	(1.45, 1.35)	(1.49, 1.32)

Results

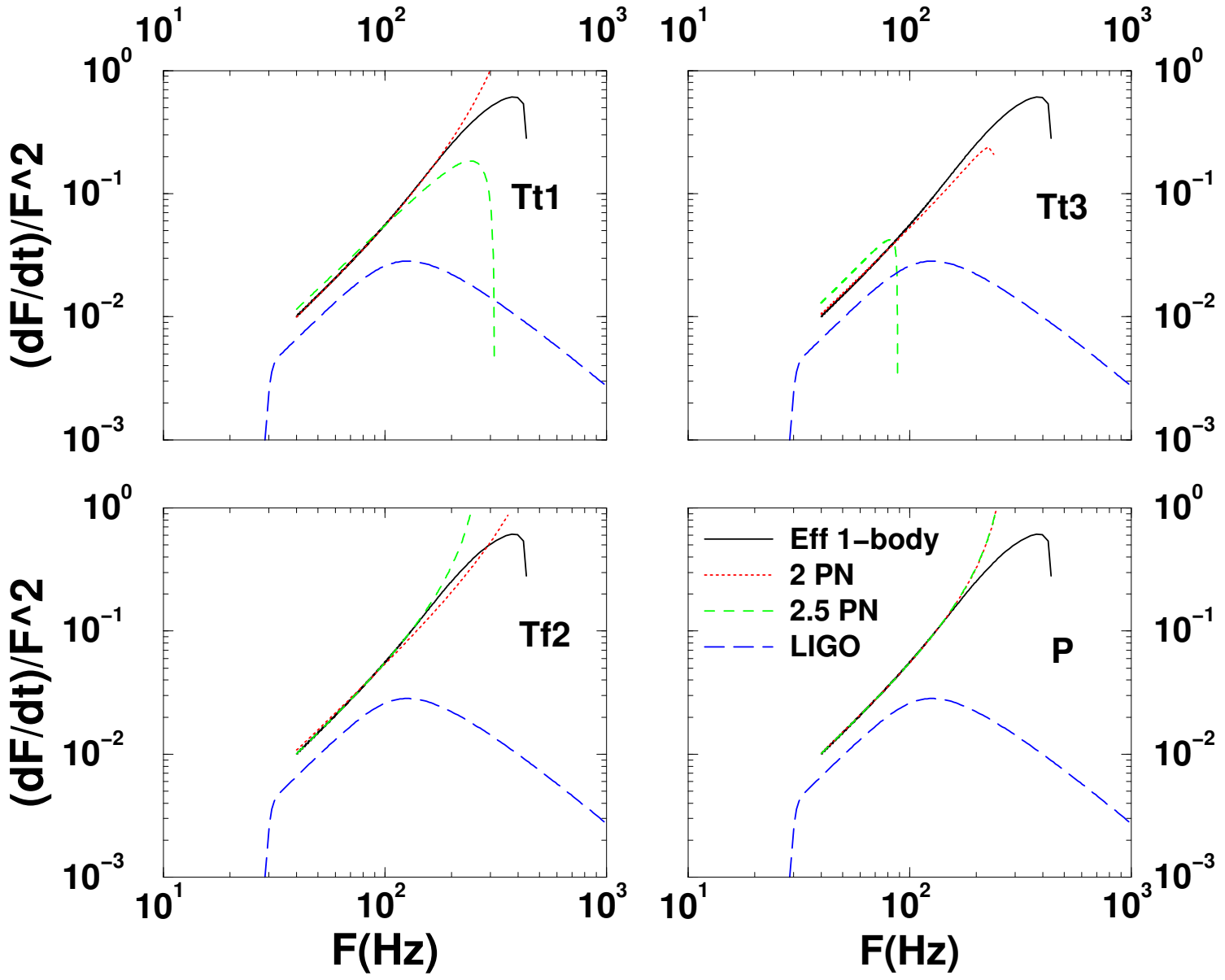

Results

- The frequency evolution ($\dot{F}/F^2$) of the various approximate models is compared with the fiducial exact $(10, 10)M_\odot$ model in the LIGO band. To indicate the effect on the overlap, we also plot the weighting function $1/h_n(f)$ for initial LIGO (not to scale), which is a measure of the detector's sensitivity.

Results

- For approximate models we exhibit the frequency evolution of the system that achieves the maximum overlap. The maximum overlap is obtained for template parameters such that the intrinsic frequency evolution of the template waveform is "tangent" to the exact one, near the maximum sensitivity of the detector.
- This can always be achieved by fitting the mass parameters. The question is whether such a local "tangency" ensures a sufficiently good "global" agreement.
- $T^{\mathrm{t}1,3}$ 2.5 PN models fare poorly in *globally* mimicking the frequency evolution of the exact waveform. This is consistent with their returning the worst overlaps of all.
- Even though the T^{f2} models do not reproduce the exact model over as large a range as the P-approximants, they achieve nearly as large overlaps as the P-approximants, because they can be made (by optimizing the masses) to agree well with the exact model over most of the sensitive part of the LIGO band.

Results

- P-approximants are able to mimic the "exact" evolution the best with little bias in the masses but, being based on the adiabatic approximation, they fail to capture the smooth transition to plunge
- Filters using the effective one-body approach go beyond the adiabatic approximation and include a smooth transition to plunge and merger. They, therefore, supersede the adiabatic-limited P-approximants. This difference between the two re-summed versions of binary signal models is important for masses larger than about 20 $M_{\odot}$.

Results

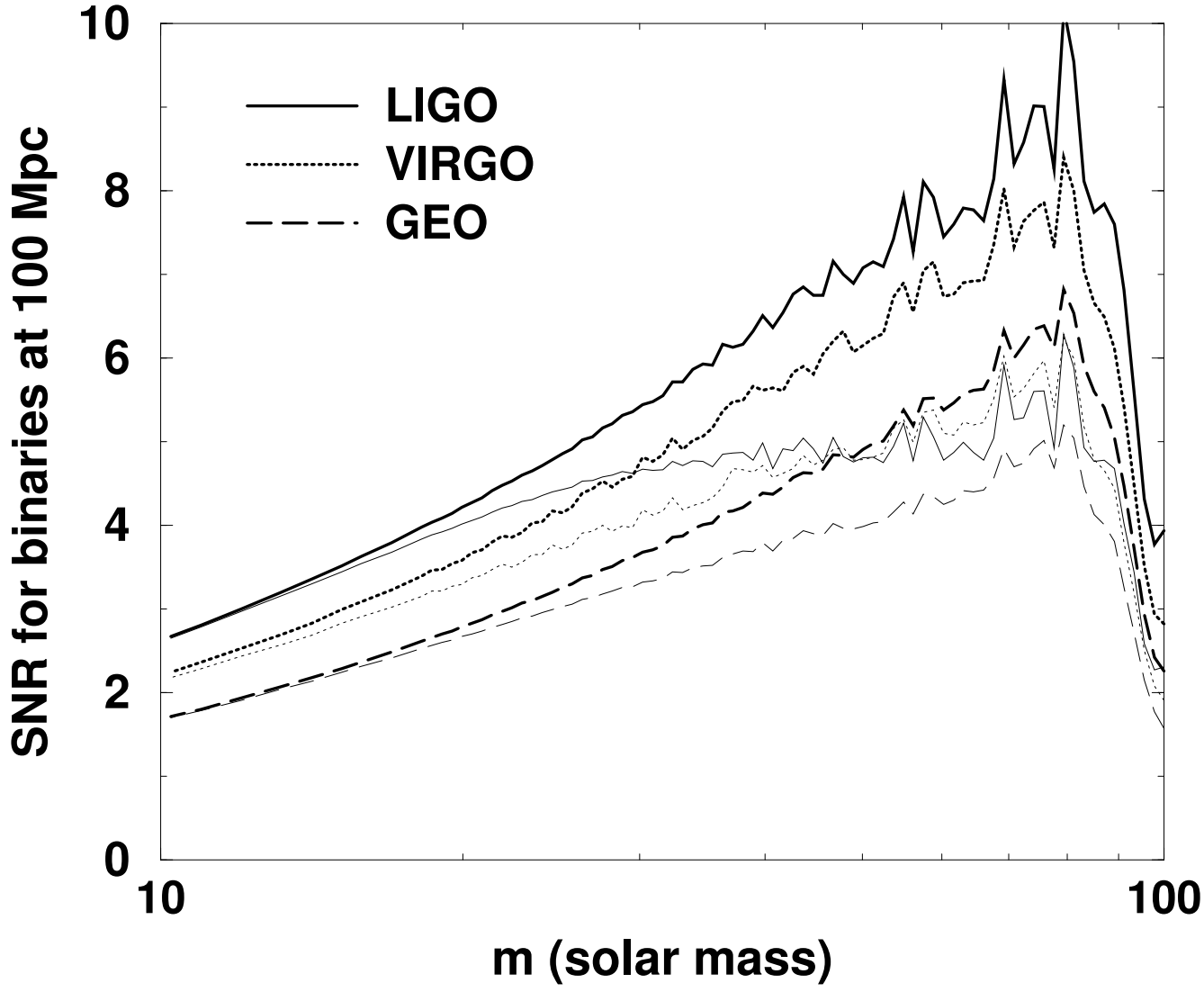
LIGO
VIRGO
GEO
SNR for binaries at 100 Mpc
m (solar mass)
0
2
4
6
8
10
10
100

Results

- Signal-to-noise ratios in GEO, LIGO-I and VIRGO when using as Fourier-domain template the post-Newtonian model (T^{f2}), truncated at the test-mass $F_{\rm lso} = 4400 M_\odot/m$ Hz (in thin lines), compared to the optimal one obtained when the template coincides with the fiducial "exact" (effective one-body) signal (thick lines). As usual, we averaged over all the angles. The overlaps are maximised over the time lags, the phases, and the two individual masses m_1 and m_2. The plots are jagged because we have computed the SNR numerically by first generating the fiducial "exact" waveform in the time-domain and thenusing its discrete Fourier transform. The greater SNR achieved by effective one-body waveforms for higher masses, is due to the plunge phase present in these waveforms. Observe that the presence of the plunge phase in the latter significantly (up to a factor of 1.5) increases the SNR for masses $m > 35 M_\odot$. Using the effective one-body templates will, therefore, enhance the search volume of the interferometric network by a factor of 3 or 4.

Inspiral, Detector Span

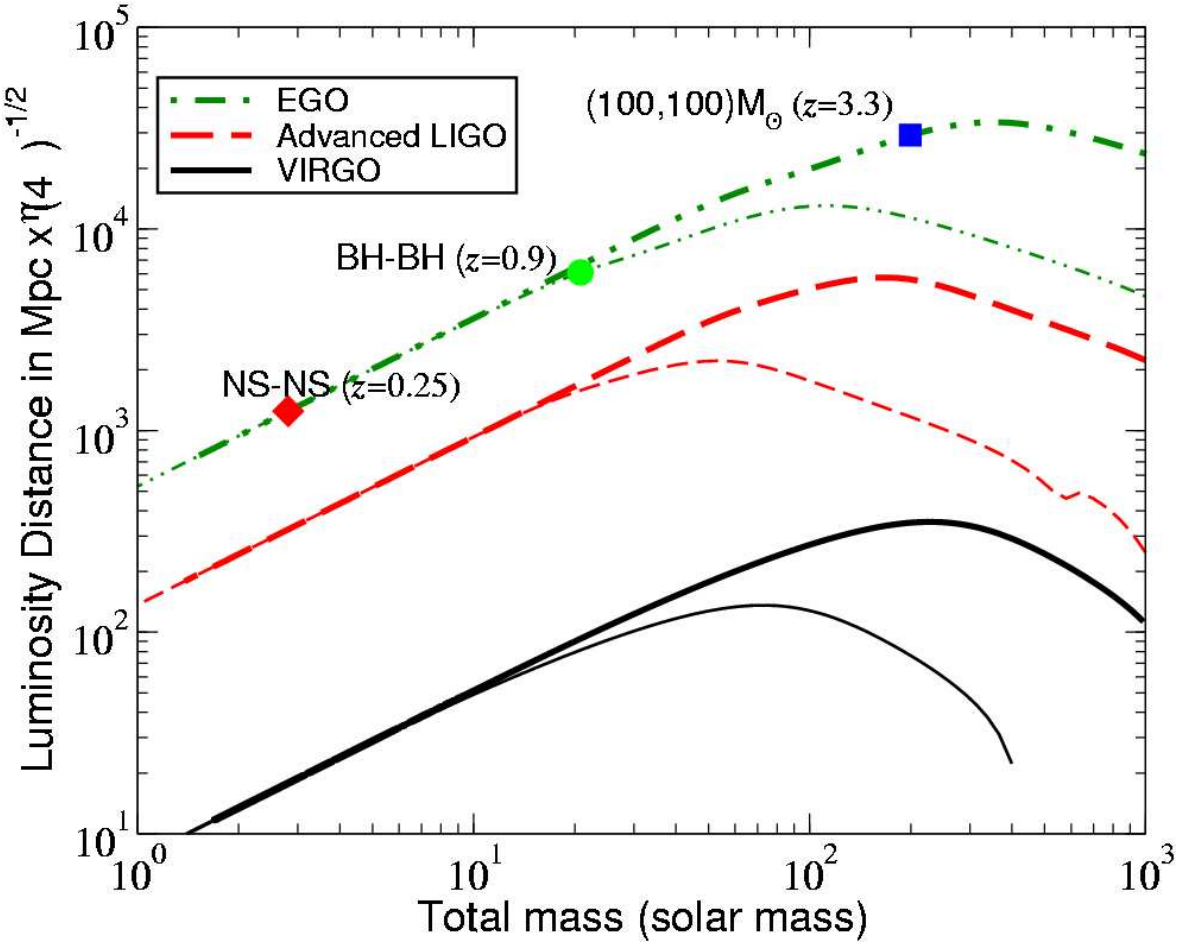

Thick Lines: EOB WF

Thin Lines: Only Inspiral

From B.S. Sathyaprakash

Buonanno, Chen Vallisneri 03

- In connection with BH-BH where one needs to go as close to the LSO as possible Buonanno Chen and Vallisneri constructed a phenomenological template by a careful study of various possible models
- Post–Newtonian models of two-body dynamics defined by BCV are given the Tables below. The notation X$(n\mathrm{PN}, m\mathrm{PN}; \hat{\theta})$ denotes the model X, with terms up to order nPN for the conservative dynamics, and with terms up to order mPN for radiation-reaction effects; for $m \geq 3$ they also needed to specify the arbitrary flux parameter $\hat{\theta}$. Now this is no longer arbitrary. For $n \geq 3$, the effective-one-body models need also two additional parameters $\tilde{z}_1$ and $\tilde{z}_2$

Buonanno, Chen Vallisneri 03

model	shorthand	evolution equation
adiabatic model with Taylor-expanded energy $\mathcal{E}(v)$ and flux $\mathcal{F}(v)$	T$(n\mathrm{PN}, m\mathrm{PN}; \hat{\theta})$	energy-balance equation
adiabatic model with Padé-expanded energy $\mathcal{E}(v)$ and flux $\mathcal{F}(v)$	P$(n\mathrm{PN}, m\mathrm{PN}; \hat{\theta})$	energy-balance equation
adiabatic model with Taylor-expanded energy $\mathcal{E}(v)$ and flux $\mathcal{F}(v)$ in the stationary-phase approximation	SPA$(n\mathrm{PN} \equiv m\mathrm{PN})$	energy-balance equation in the freq. domain
nonadiabatic Hamiltonian model with Taylor-expanded GW flux	HT$(n\mathrm{PN}, m\mathrm{PN}; \hat{\theta})$	Hamilton equations

Buonanno, Chen Vallisneri 03

model	shorthand	evolution equation
nonadiabatic Hamiltonian model with Padé-expanded GW flux	HP$(n\mathrm{PN}, m\mathrm{PN}; \hat{\theta})$	Hamilton equations
nonadiabatic Lagrangian model	L$(n\mathrm{PN}, m\mathrm{PN})$	$\mathbf{F} = m\mathbf{a}$
nonadiabatic effective-one-body model with Taylor-expanded GW flux	ET$(n\mathrm{PN}, m\mathrm{PN}; \hat{\theta}; \tilde{z}_1, \tilde{z}_2)$	eff. Hamilton equations
nonadiabatic effective-one-body model with Padé-expanded GW flux	EP$(n\mathrm{PN}, m\mathrm{PN}; \hat{\theta}; \tilde{z}_1, \tilde{z}_2)$	eff. Hamilton equations

What is it about?

- There are at least three different contexts in which one can examine the performance of an approximate template family relative to an exact one.
- Firstly, one can think of a mathematical family of approximants and examine its convergence towards some exact limit.
- Secondly, one can ask whether this mathematical family of approximants correctly represents the GWs from some physical system.
- Thirdly, how does this family of approximate templates converge to the exact solution in the sensitive bandwidth of a particular GW detector.
- In the context of GWDA, the third context will be relevant.
- Although there is no direct application to GW data analysis, equally interesting is the mathematical question concerning the behavior of different approximations, and the waveforms they predict, in the strongly non-linear regime of the dynamics of the binary. The latter obviously does not require the details of the detector-sensitivity and it is enough to study the problem assuming a flat power spectral density (i.e. a *white-noise* background) for the detector noise.

Issues Related to WF Modelling

Model for the orbit: Circular vs Elliptic

Ref: Arun (PhD Thesis 2006 - Unpublished)

- We list the most important issues in modelling ICB and the progress made in addressing them.
- For nonspinning binaries in quasi-circular orbits of arbitrary mass ratio, up to 3.5PN in the phase and 2.5PN in the amplitude. Though the 1.5PN and 2PN phasing may not be good enough for an accurate detection and parameter estimation, the 3.5PN should be reasonably accurate for the purpose.
  Data analysis strategies for the eccentric binaries are more involved.

Spin of the binary: Spinning vs Nonspinning

- Though one may argue that the spin effects are more important for binaries with large mass ratio, including the spin effects is an important step towards constructing more realistic and general templates. Theoretically, computation of waveforms with spin effects is more complex. Till date spin effects are computed in the phase up to 2.5PN order (Apostolatos et al 94; Kidder Will Wiseman 93; Kidder 95; Blanchet Buonanno Faye 06) and in the amplitude up to 2PN order (Kidder 95,Ohashi Tagoshi Owen 98). Apostolatos et al gave a prescription to incorporate orbital precession effects and the consequent modulations in the model of the gravitational waveform.

Issues Related to WF Modelling

Restricted WF vs Full WF

- GWDA uses `restricted waveform approximation'. Very high PN accurate phasing of the binary, keeping the amplitude of the wave to be at leading Newtonian order. This is justified by the argument that matched filtering is more sensitive to the phase of the GW than its amplitude.
  There have been investigations by Van Den Broeck 06; Van Den Broeck, Sengupta 06; about the validity of the restricted waveform approximation in the detection as well as parameter estimation. Evaluated the differences arising by the use of the non-restricted waveform in both detection as well as parameter estimation. The overestimation in SNR by the restricted waveform templates due to the absence of higher harmonics have to be accounted for while constructing the templates for data analysis

Issues Related to WF Modelling

Late inspiral: Adiabatic vs Non-adiabatic

- Computation of the waveforms for the inspiralling compact binary systems are implemented using the PN approximation to general relativity. One assumes here that though the orbital frequency of the system changes with time, the change in frequency per orbital period is negligible compared tothe orbital frequency itself, i.e., $\frac{\dot{\omega}}{\omega^2} \ll 1$. Strictly speaking, this *adiabatic approximation* is valid only in the early part of the inspiral and not during the very late inspiral and merger phases. Hence the standard PN approximation is expected to break down towards the very late part of the inspiral.
- Alternatives have to be explored to include the effects of non-adiabaticity and to model the plunge and merger phases. Effective one body (EOB) approach first proposed by Buonanno and Damour is one of the most important among them. This method, for the first time, does not assume adiabaticity anymore and provides an analytical description of the transition from plunge to merger and subsequent 'ringing'. 3PN: Damour Jaranowski Schäfer; Spin EOB: Damour 01

Issues Related to WF Modelling

Late inspiral: Adiabatic vs Non-adiabatic

- Other approaches to go beyond the adiabatic approximation, have been made by Buonanno, Chen, Vallisneri, Pan.. and Ajith , Iyer, Robinson, Sathyaprakash
- With the recent progresses in numerical relativity, there is hope that one will have better waveforms for the late inspiral and merger parts of the binary evolution which can be used for constructing templates as well as to test the robustness of the analytical adiabatic and non-adiabatic models. Pretorius 05, Baker et al 06, Campanelli et al 06, Herman et al 06; Sperhake 06; Buonanno, Cook, Pretorius 06; Damour, Nagar 06.....

To ReSum or not ReSum? Padé vs Taylor

Is the two-body problem in GR Schwarzschild like?

- While advocates of Resummation are convinced of its necessity and the inadequacy of a simple PN expansion near the ISCO critics of these approximants have a different view
- The usual objection raised is `It accelerates convergence..But how does one know it converges to the correct limit of GR?'
- The only concrete discussion of this is by Blanchet .. See Living review for an updated discussion..Some arguments e.g. are:
- Values of the ambiguity parameter predicted by convergence arguments of resummed approximants were incorrect
- The ratio of diff PN order coeffs is related to the Radius of convergence of the PN series which is determined by the location of the light ring
- The two-body interaction in GR may not be Schwarzschild-like. There may be no light ring unlike the test mass case and hence the resummed approximants based on this implicit closeness to the test mass case, could predict very different higher order PN coeffs from resummation than the true GR ones
- PN series is an asymptotic series and 3PN is accurate enough even at the ISCO
- Talks by Damour, Nagar for the opposite viewpoint

Issues Related to WF Modelling

Non-Restricted Full Waveform

- Recently Van Den Broeck and Sengupta have looked at the implications of the Full Waveform rather than the Restricted WF for DA
- The waveforms in the two polarizations take the general form

$$h_{+,\times} = \frac{2M\eta}{r} x \left\{ H^{(0)}_{+,\times} + x^{1/2} H^{(1/2)}_{+,\times} + x H^{(1)}_{+,\times} + x^{3/2} H^{(3/2)}_{+,\times} + x^2 H^{(2)}_{+,\times} + x^{5/2} H^{(5/2)}_{+,\times} \right\}$$

- Coefficients $H^{(n/2)}_{+,\times}$, $n = 0, \ldots, 5$, are linear combinations of various harmonics with prefactors that depend on the inclination angle $\imath$ of the angular momentum of the binary with respect to the line of sight as well as on η(ABIQ). Measured signal also depends on the polarization angle and the position in the sky through the detector's beam pattern functions $F_{+,\times}$:

$$h(t) = F_+ h_+(t) + F_\times h_\times(t).$$

- For ground-based detectors, it is reasonable to approximate $F_{+,\times}$ as being constant over the duration of the signal. They depend on angles (θ, ϕ, ψ), where (θ, ϕ) determine sky position while ψ is the polarization angle. The signal is a linear combination of harmonics of the orbital phase $\Psi(t)$ with offsets $\varphi_{(k,m/2)}$:

Issues Related to WF Modelling

Non-Restricted Full Waveform

$$h(t) = \sum_{k=1}^{N_p} \sum_{m=0}^{2p} A_{(k,m/2)}(t) \cos(k\Psi(t) + \varphi_{(k,m/2)}),$$

- Coefficients $A_{(k,m/2)}$ are functions of $(r, M, \eta, \theta, \phi, \psi, \imath)$ multiplied by $x^{(m+2)/2}$. Orbital phase $\Psi(t)$ is a series in x, which for non-spinning binaries is known to 3.5PN order. The number of harmonics N_p depends on the PN order in amplitude, p; at 2.5PN one has $N_p = 7$.
- The SPA for the $(p, 3.5)$PN waveform is then

$$\tilde{h}_{SPA}(f) = \sum_{k=1}^{N_p} \left[\frac{\sum_{m=0}^{2p} A_{(k,m/2)} \left(t\left(\frac{1}{k}f\right)\right) e^{-i\varphi_{(k,m/2)}}}{2\sqrt{k\dot{F}\left(t\left(\frac{1}{k}f\right)\right)}} \right]_p \exp\left[i \left(2\pi f t_c - \pi/4 + k\psi \right.\right.$$

$[\,.\,]_p$ denotes consistent truncation to pth post-Newtonian order (i.e., the "Newtonian" prefactor $f^{-7/6}$ is taken outside and the remaining expression is expanded in $(2\pi M f)^{1/3}$ up to $(2\pi M f)^{2p/3}$).

Issues Related to WF Modelling

Non-Restricted Full Waveform

- If h is $(p, 3.5)$PN Full WF and h_0 the correspg restricted $(0, 3.5)$PN WF they get

	NS–NS		NS–BH		BH–BH	
p	$\rho[h_0]$	$\rho[h]$	$\rho[h_0]$	$\rho[h]$	$\rho[h_0]$	$\rho[h]$
0	6.465	6.465	13.492	13.492	30.928	30.928
0.5	"	6.465	"	13.932	"	30.928
1	"	6.286	"	12.563	"	28.135
1.5	"	6.286	"	12.421	"	28.135
2	"	6.249	"	12.090	"	26.373
2.5	"	6.247	"	12.002	"	26.285

Table 1: Change in signal-to-noise ratios with increasing p in $(p, 3.5)$PN waveforms, for three different systems at 20 Mpc. (Angles were chosen arbitrarily as $\theta = \phi = \pi/6, \psi = \pi/4, \imath = \pi/3$.)

- Though $\rho(h)$ or $\rho(h_0)$ depend on the choice of angles their relative difference has only a weak dependence on angles

Non-Restricted Full Waveform - Mass reach

Advanced LIGO

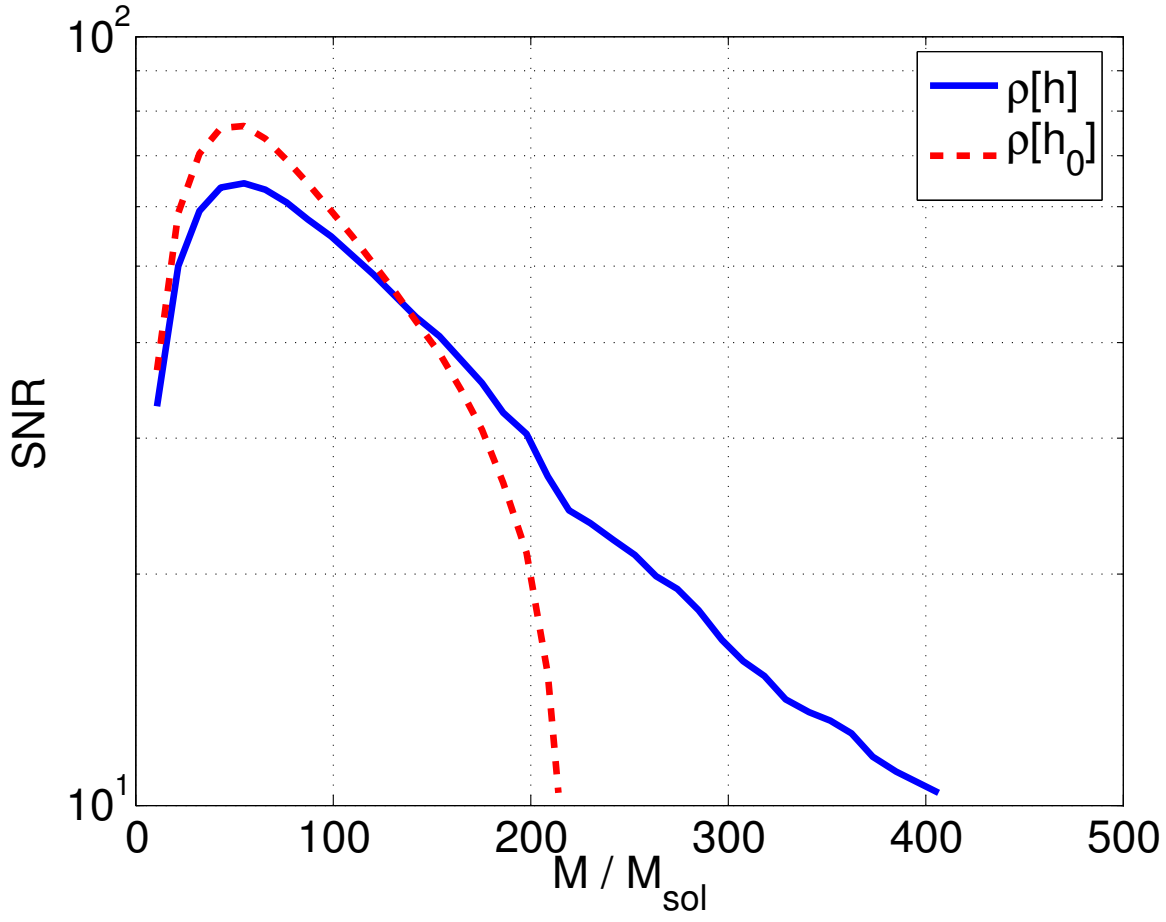

Non-Restricted Full Waveform - Mass reach

EGO

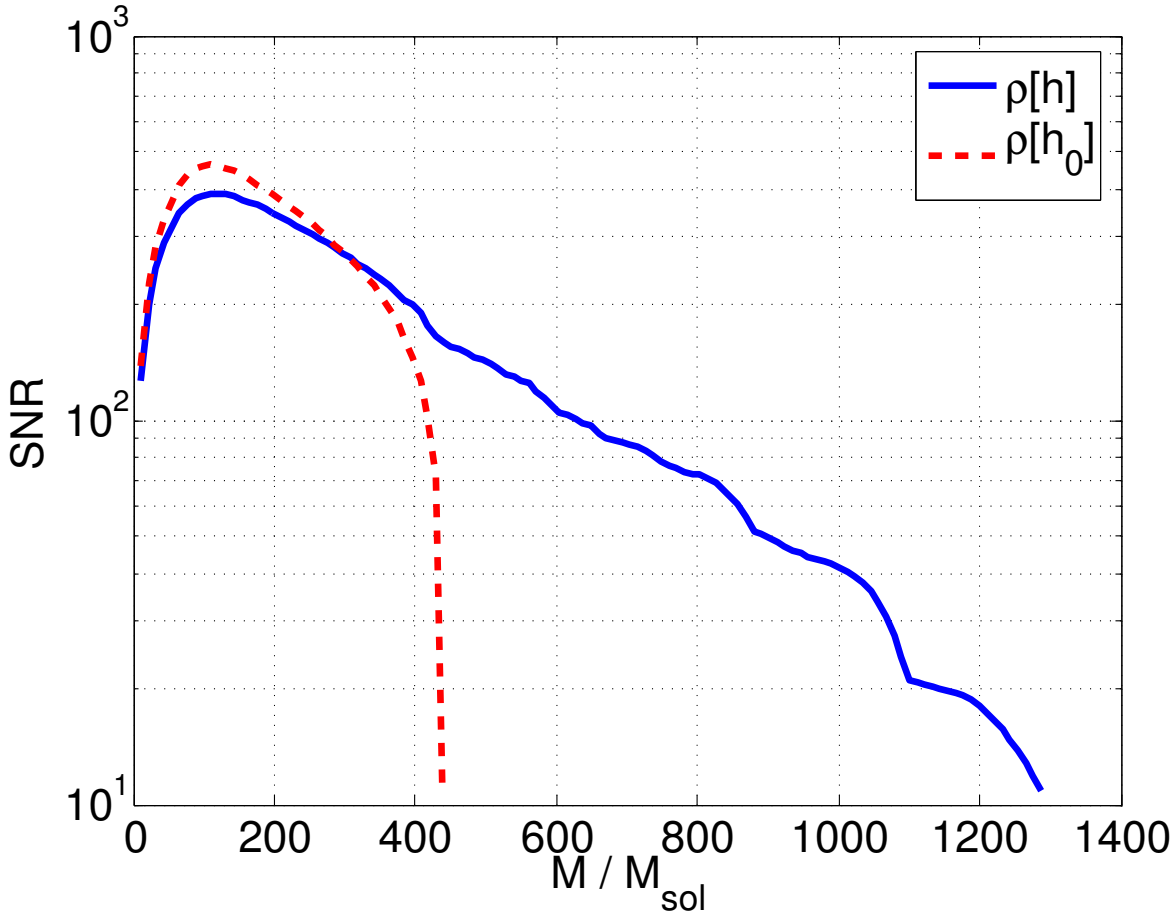

Non-Restricted Full Waveform - Mass reach

Plots of $\rho[h]$ and $\rho[h_0]$ as functions of total mass for Advanced LIGO and EGO. Distance is fixed at 100 Mpc, and we assume $m_1/m_2 = 0.1$. Angles are as earlier. At low masses one has $2f_{LSO} \gg f_s$ and $\rho[h_0]$ dominates. For sufficiently high masses, $2f_{LSO} \leq f_s$, so that the dominant harmonic no longer enters the detector's bandwidth and the SNR for the restricted waveform vanishes. For such masses, higher harmonics in the amplitude-corrected waveform will continue to enter the bandwidth and can lead to significant SNRs. As a result, at the given distance the use of amplitude-corrected waveforms approximately doubles the mass reach of Advanced LIGO and triples that of EGO.

Non-Restricted Full Waveform - Mass reach

Advanced LIGO

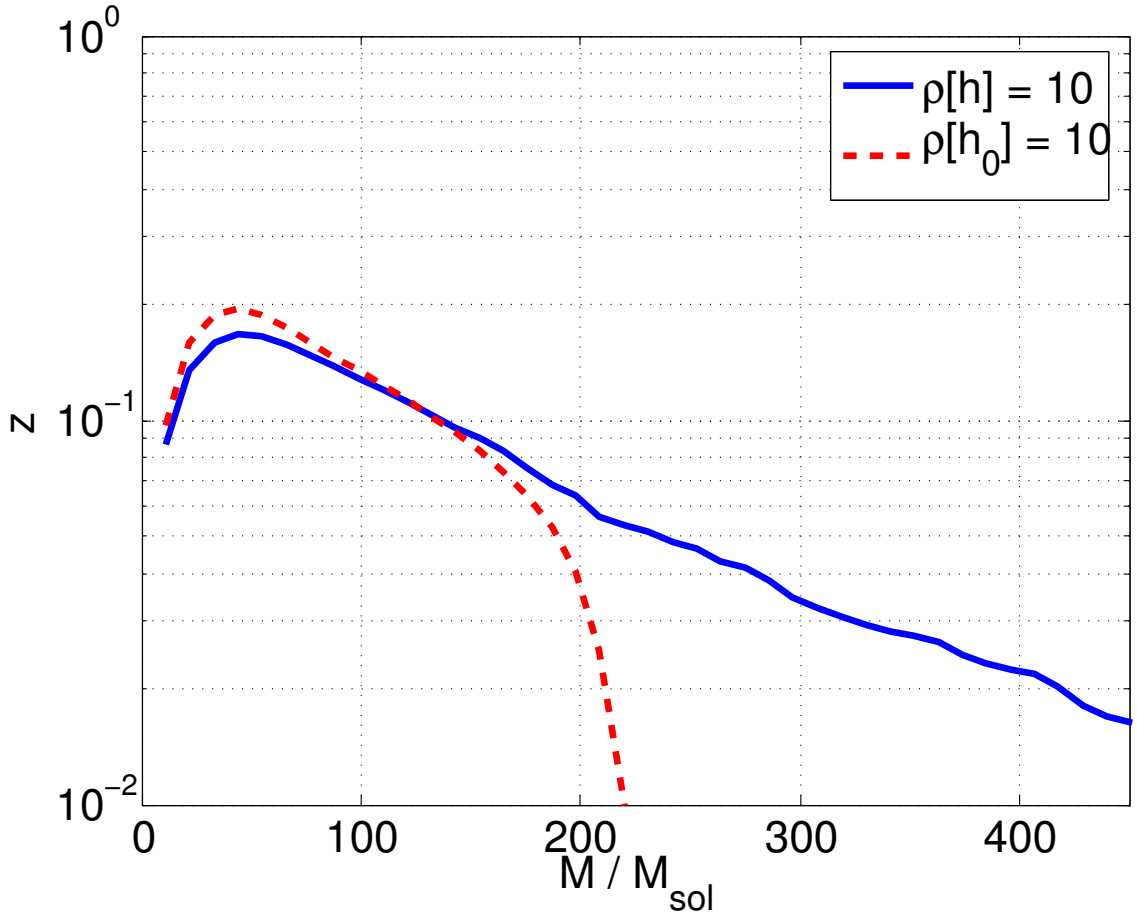

Non-Restricted Full Waveform - Mass reach

EGO

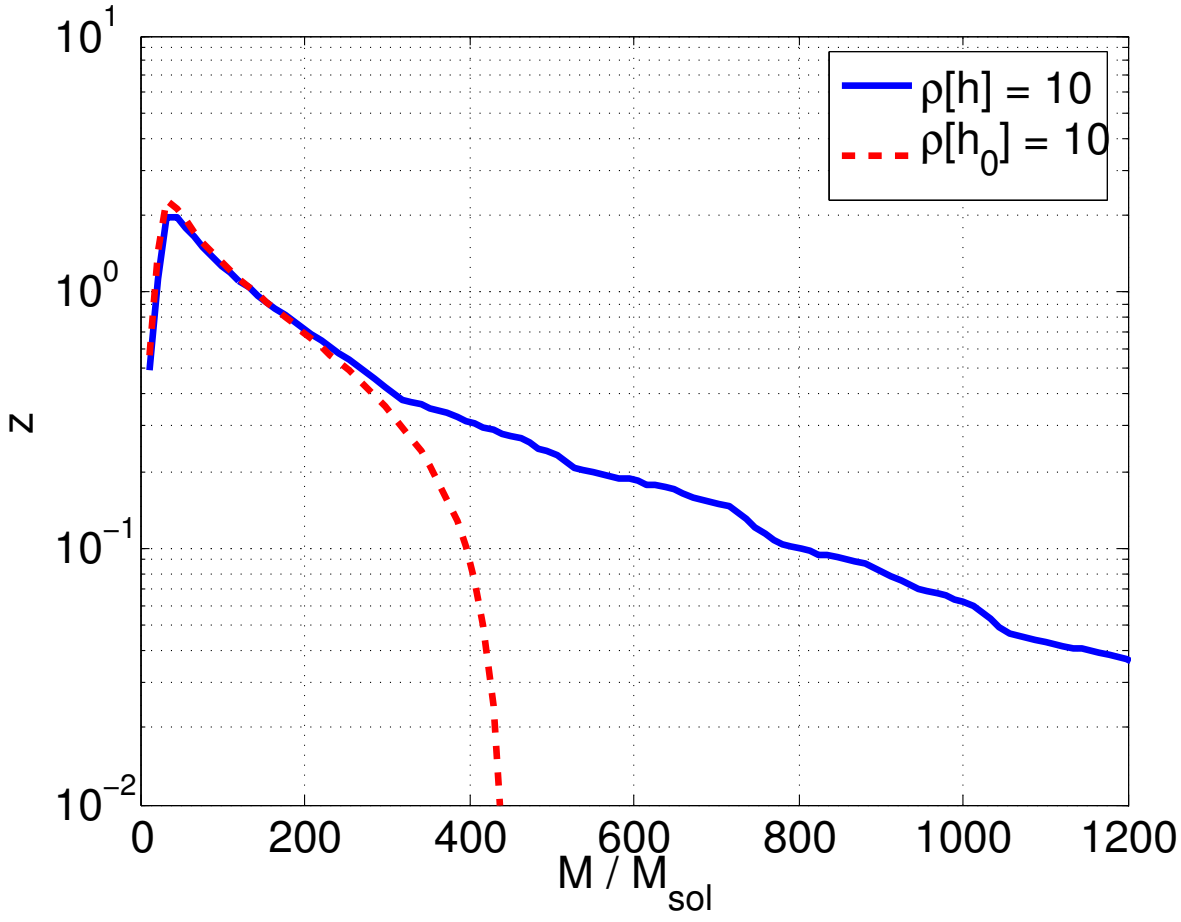

Non-Restricted Full Waveform - Mass reach

The redshift reach of Advanced LIGO and EGO as functions of (physical) total mass for fixed SNRs of 10 with amplitude-corrected and restricted waveforms. We have fixed $m_1/m_2 = 0.1$, and angles are as before

Issues Related to WF Modelling

Non-Restricted Full Waveform

- For initial detectors modelling signals as restricted generally leads to overestimates of SNR
- This is because of `destructive' interference between harmonics
- Advanced detectors will be sensitive at lower frequencies and higher harmonics may enter BW even if the dominant one does not. Detector's mass reach may increase by factors of two (adv LIGO) or three (EGO). Allow for detection of inspirals with higher total mass.

PART II

New Class of post-Newtonian Waveform Templates for Inspiralling Compact Binaries

Based on

P. Ajith, B. R. Iyer, C. A. K. Robinson and
B S Sathyaprakash

Phys. Rev. D **71**, 044029 (2005)

Standard Adiabatic Approximnts

- The *standard adiabatic* approximation to phasing uses the energy and flux functions to *same relative* PN accuracy
- Including the radiation reaction at dominant order, however, is not a first order correction to the *dynamics* of the binary, but rather the 2.5PN order correction
- Thus the phasing of the GW, when viewed in terms of the underlying dynamics is described as motion under the dominant Newtonian force and a perturbation/correction at order $(v/c)^5$, *neglecting* the intermediate conservative force terms at 1PN $(v/c)^2$ and 2PN $(v/c)^4$ orders

Standard Non-Adiabatic Models

- Latter Point more Transparent in phasing models constructed explictly from the EOM: *Non-Adiabatic Approximants*
- *Lagrangian* templates studied by Buonanno, Chen and Vallisneri (BCV) can be thought of as examples of *standard non-adiabatic* approximants since to reproduce *standard phasing* it only retains associated 'acceleration' terms as mentioned earlier resulting in 'gaps' in the acceleration

Standard Non-Adiabatic ... Contd

- The Lagrangian models studied by BCV are specified by the relative acceleration of the binary system

$$\frac{d\mathbf{x}}{dt} = \mathbf{v}\,; \quad \frac{d\mathbf{v}}{dt} = \mathbf{a}$$

$$\frac{d\phi}{dt} = \omega\,; \quad v^2 = r^2\omega^2; \quad \varphi = 2\phi$$

- Accn is given as a PN expansion
- 0PN: $\mathbf{a} = \mathbf{a}_{\rm N} + \mathbf{a}_{\rm 2.5PN}$
- 1PN: $\mathbf{a} = \mathbf{a}_{\rm N} + \mathbf{a}_{\rm 1PN} + \mathbf{a}_{\rm 2.5PN} + \mathbf{a}_{\rm 3.5PN}$
- Missing intermediate PN terms in the acceleration

Complete Non-Adiabatic Models

- Consistently includes *all* acceleration terms *up to* relevant PN order
- 0PN: $\mathbf{a} = \mathbf{a}_{\rm N} + \mathbf{a}_{\rm 1PN} + \mathbf{a}_{\rm 2PN} + \mathbf{a}_{\rm 2.5PN}$
- 1PN: $\mathbf{a} = \mathbf{a}_{\rm N} + \mathbf{a}_{\rm 1PN} + \mathbf{a}_{\rm 2PN} + \mathbf{a}_{\rm 2.5PN} + \mathbf{a}_{\rm 3PN} + \mathbf{a}_{\rm 3.5PN}$

Complete Adiabatic Approxmts

- In the *adiabatic* approximation the Energy function codes information about PN conservative dynamics while the Flux function codes the dissipative dynamics due to GRR
- A new and simple *complete adiabatic approximant* is proposed constructed from the Energy and Flux functions
- Given the 0PN flux (leading to $\mathbf{a}_{2.5\mathrm{PN}}$), we choose the Energy function at 2PN ($\sim$ 2PN conservative dynamics) rather than to the *standard* choice of 0PN ($\sim$ 0PN or Newtonian dynamics).

Complete Adiabatic Approxmts

- Given the Flux at n-PN, a corresponding complete adiabatic approximant is constructed by choosing the Energy Fn at order $[n + 2.5]$PN, where $[p]$ denotes the integer part of p.
- The *complete* adiabatic approximant in spirit corresponds to dynamics where there are no missing PN terms in the acceleration
- *Caveat*: Unique only without Further *re-expansions* of the Energy and Flux functions during evaluation of Phasing Formula

Test Mass Exact Waveform

- For a test-particle orbiting the Schwarzschild BH the Energy function and Flux function are known Exactly (former analytically, latter numerically (Poisson)).
  A natural fiducial 'signal' or ' Exact' waveform is thus available to compare different template models
- The Flux function is also analytically known to a very high 5.5PN order (Tanaka, Tagoshi and Sasaki) making possible construction of many *standard* and *complete adiabatic* approximant templates

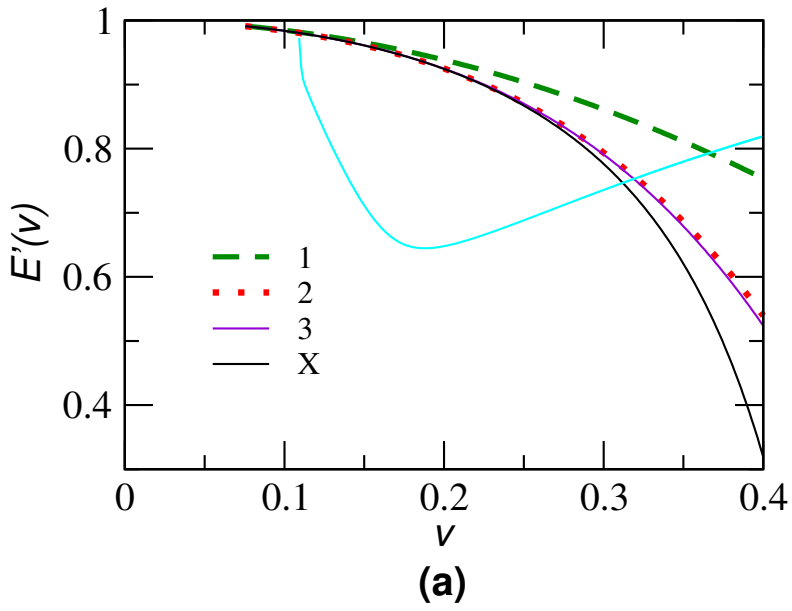

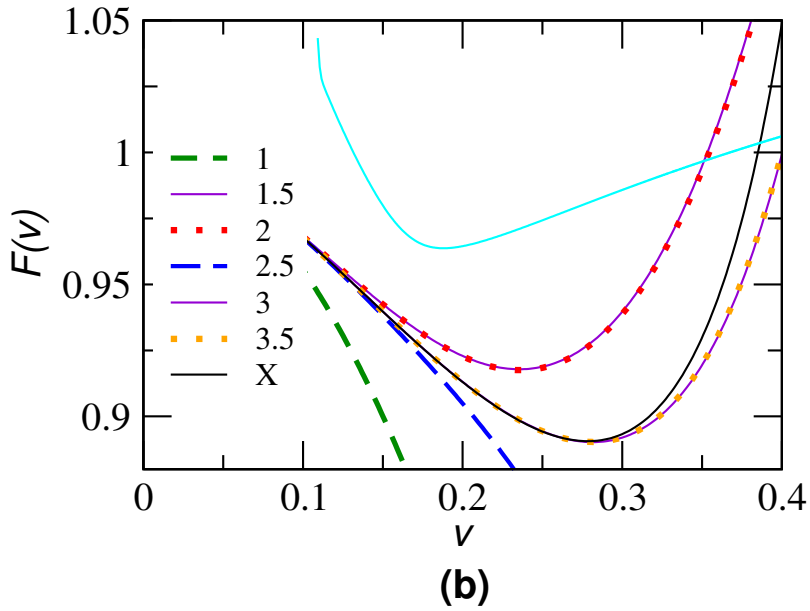

PN Approximants of the Energy and Flux Functions and their Approach to Exact Energy and Flux Functions

$$E_{\rm exact} = \eta \frac{1-2v^2}{\sqrt{1-3v^2}}; \quad \eta = \frac{\mu}{m} = \frac{m_1 m_2}{m^2}$$

Present Work

- Using the exact/approximate energy and flux functions, the exact/approximate waveforms are constructed by the relevant phasing formula
- Overlaps of the *standard* and *complete adiabatic* approximant templates with the Exact waveform are compared to gauge their their performance
- Performance is quantified by twin notions of *effectualness* and *faithfulness*
- Binaries studied:
  $(1M_\odot, 10M_\odot)$, $(1M_\odot, 50M_\odot)$ $(1M_\odot, 100M_\odot)$

Present Work ... Contd

- Overlaps first calculated assuming a flat power spectral density for detector noise (*white noise*):
  a mathematical question concerning convergence properties of the PN waveform family independent of detector properties
- Overlaps next calculated for initial LIGO, VIRGO and Advanced LIGO

Effectualness: White N (Adiabatic)

	$(1M_\odot, 10M_\odot)$				$(1M_\odot, 50M_\odot)$		
	TaylorT1		*TaylorF1*		*TaylorT1*		
Order (n)	*S*	*C*	*S*	*C*	*S*	*C*	*S*
0PN	0.6250	0.8980	0.6212	0.8949	0.5809	0.9726	0.59
1PN	0.4816	0.5119	0.4801	0.5086	0.4913	0.9107	0.48
1.5PN	0.9562	0.9826	0.9448	0.9592	0.9466	0.9832	0.93
2PN	0.9685	0.9901	0.9514	0.9624	0.9784	0.9917	0.97
2.5PN	0.9362	0.9924	0.9298	0.9602	0.7684	0.9833	0.73
3PN	0.9971	0.9991	0.9677	0.9713	0.9861	0.9946	0.98
3.5PN	0.9913	0.9996	0.9636	0.9688	0.9902	0.9994	0.98
4PN	0.9937	0.9973	0.9643	0.9663	0.9975	0.9996	0.99
4.5PN	0.9980	0.9999	0.9671	0.9690	0.9967	1.0000	0.99
5PN	0.9968	0.9979	0.9661	0.9667	0.9994	0.9994	0.99

Results: White Noise (Adiabatic)

- Complete adiabatic approximants lead to a remarkable improvement in the effectualness (i.e. larger overlaps with the 'exact' signal) at lower PN ($<$ 3PN) orders
- However, standard adiabatic approximants of orders $\geq$ 3PN are nearly as good as the complete adiabatic approximants for construction of *effectual* templates
- In general *faithfulness* of complete approximants is also better than that of standard approximants.
- There do exist *anomalous* cases where the complete approximant performs worse than the standard

Effectualness: LIGO (Adiabatic)

Percentage biases σ_m and σ_η in determining parameters m and η are given in brackets.

	$(1M_\odot, 10M_\odot)$			
	TaylorT1		*TaylorF1*	
Order (n)	*S*	*C*	*S*	
0PN	0.5910 (12, 5.7)	0.9707 (36, 45)	0.5527 (31, 28)	0.839
1PN	0.5232 (22, 105)	0.8397 (125, 69)	0.4847 (18, 9.7)	0.8393
1.5PN	0.9688 (52, 51)	0.9887 (8.3, 15)	0.8398 (61, 57)	0.860
2PN	0.9781 (18, 25)	0.9942 (0.4, 0.6)	0.8485 (32, 40)	0.869
2.5PN	0.9490 (96, 68)	0.9923 (26, 32)	0.8963 (123, 75)	0.907
3PN	0.9942 (0.3, 1.1)	0.9989 (3.7, 6.2)	0.8713 (16, 23)	0.882
3.5PN	0.9940 (6.9, 11)	0.9998 (0.6, 1.4)	0.8685 (23, 31)	0.883
4PN	0.9974 (6.2, 11)	0.9996 (3.9, 6.9)	0.8746 (23, 30)	0.881
4.5PN	0.9988 (3.3, 5.5)	1.0000 (0.8, 1.6)	0.8795 (19, 27)	0.886
5PN	0.9992 (4.0, 6.9)	0.9997 (3.5, 5.7)	0.8792 (21, 29)	0.882

Faithfulness: LIGO (Adiabatic)

	$(1M_\odot, 10M_\odot)$				$(1M_\odot, 50M_\odot)$		
	TaylorT1		*TaylorF1*		*TaylorT1*		
Order (n)	*S*	*C*	*S*	*C*	*S*	*C*	*S*
0PN	0.2186	0.6272	0.2108	0.5879	0.2134	0.3498	0.21
1PN	0.1342	0.1615	0.1308	0.1563	0.1511	0.2196	0.15
1.5PN	0.3788	0.4492	0.3449	0.6471	0.2915	0.9223	0.29
2PN	0.7449	0.7633	0.6279	0.7782	0.3613	0.8157	0.36
2.5PN	0.3115	0.3970	0.2905	0.3532	0.2608	0.4233	0.26
3PN	0.9633	0.7566	0.7913	0.8297	0.7194	0.9686	0.70
3.5PN	0.8385	0.9984	0.6582	0.7464	0.4941	0.9273	0.50
4PN	0.8356	0.8909	0.6527	0.6725	0.5960	0.7934	0.58
4.5PN	0.9395	0.9851	0.6967	0.7195	0.7594	0.9644	0.76
5PN	0.8960	0.9129	0.6770	0.6821	0.7344	0.8350	0.74

Fixed PN Flux, Varying PN Energy

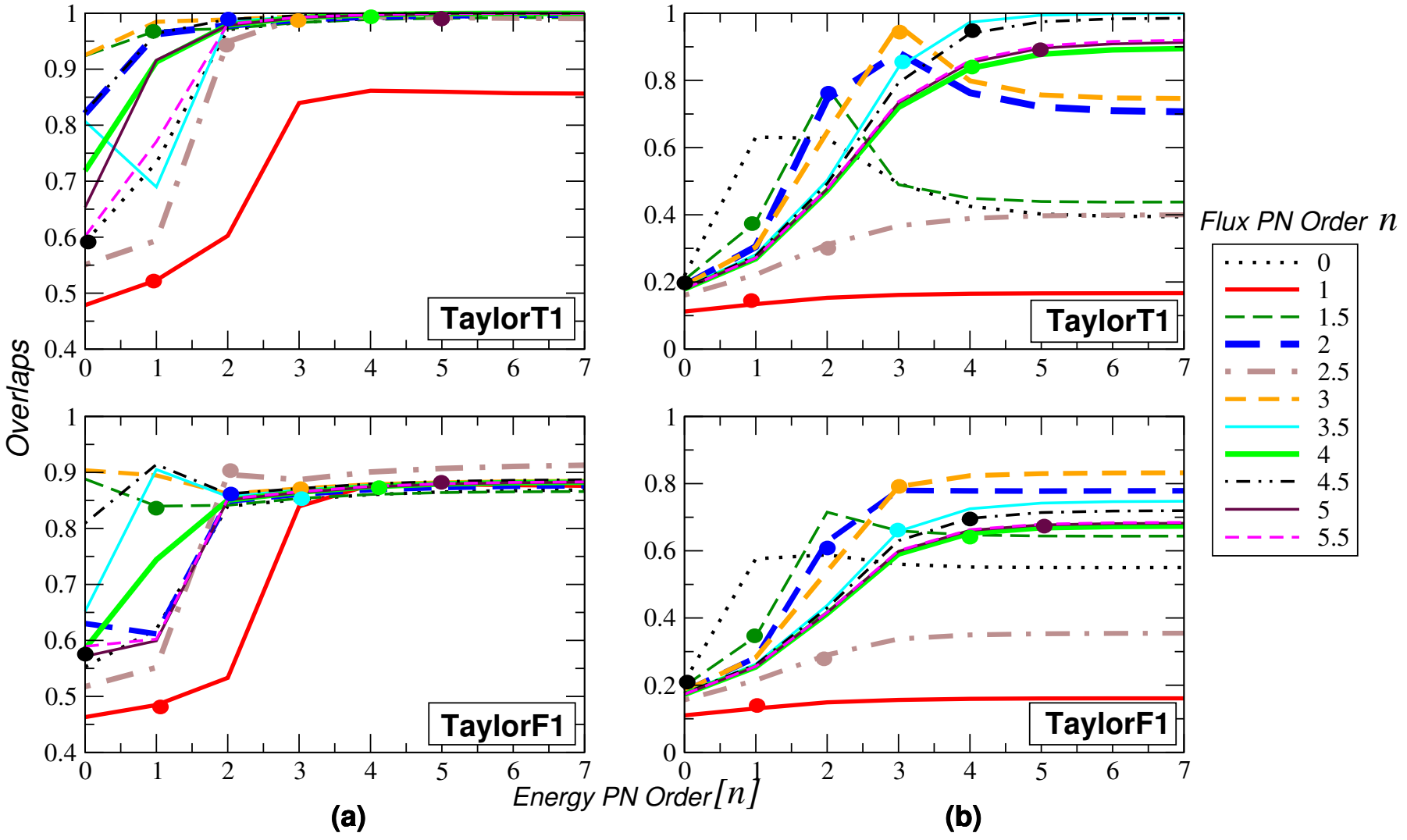

Figure details

Effectualness (left) and faithfulness (right)

TaylorT1 and *TaylorF1* templates

Initial LIGO noise PSD

Different lines $\sim$ different orders of flux function

Each line$\sim$ overlaps as fn of accuracy of energy fn

Standard adiabatic approximants $T(E_{[n]}, \mathcal{F}_n)$
are marked with thick dots.

Results: Initial LIGO, VIRGO ..

- Complete adiabatic approximants lead to a remarkable improvement in the *effectualness* at lower PN ($<$ 3PN) orders.
- However standard adiabatic approximants are nearly as good as the complete adiabatic approximants for construction of *effectual* templates
- *Faithfulness* of complete approximants is almost always better than that of standard approximants

Effectualness: (Non-Adiabatic)

Initial LIGO noise PSD.
Percentage biases σ_m and σ_η in determining parameters m and η are given in brackets.

	$(10M_\odot, 10M_\odot)$			
	TaylorT1		*TaylorF1*	
Order (n)	*S*	*C*	*S*	
0PN	0.8818 (14, 0.0)	0.9503 (3.6, 0.0)	0.8813 (11, 0.0)	0.9485
1PN	0.8453 (59, 0.1)	0.8944 (45, 10)	0.8088 (52, 0.0)	0.862
1.5PN	0.9535 (3.9, 0.3)		0.9735 (22, 29)	
2PN	0.9846 (0.1, 0.6)		0.9757 (0.7, 0.1)	
2.5PN	0.8803 (9.4, 0.1)		0.9412 (35, 35)	
3PN	0.9838 (1.4, 0.0)		0.9751 (1.2, 0.1)	
3.5PN	0.9832 (1.3, 0.0)		0.9751 (1.2, 0.1)	

Faithfulness: (Non-Adiabatic) - Test Mass

Initial LIGO noise PSD.

	$(1M_\odot, 10M_\odot)$		$(1M_\odot, 50M_\odot)$	
Order (n)	S	C	S	C
0PN	0.2463	0.1216	0.5048	0.1747
1PN	0.4393	0.1823	0.3650	0.3119

Effectualness: NonAdiabatic - Comparable Masses

Initial LIGO noise spectrum.
Percentage biases σ_m and σ_η in determining parameters m and η are given in brackets.

	$(10M_\odot, 10M_\odot)$			
	TaylorT1		*TaylorF1*	
Order (n)	*S*	*C*	*S*	
0PN	0.8818 (14, 0.0)	0.9503 (3.6, 0.0)	0.8813 (11, 0.0)	0.9485
1PN	0.8453 (59, 0.1)	0.8944 (45, 10)	0.8088 (52, 0.0)	0.862
1.5PN	0.9535 (3.9, 0.3)		0.9735 (22, 29)	
2PN	0.9846 (0.1, 0.6)		0.9757 (0.7, 0.1)	
2.5PN	0.8803 (9.4, 0.1)		0.9412 (35, 35)	
3PN	0.9838 (1.4, 0.0)		0.9751 (1.2, 0.1)	
3.5PN	0.9832 (1.3, 0.0)		0.9751 (1.2, 0.1)	

Faithfulness: NonAdiabatic - Comparable Mases

Initial LIGO noise spectrum.

	$(10M_\odot, 10M_\odot)$				$(1.4M_\odot, 1.4M_\odot$		
	TaylorT1		*TaylorF1*		*TaylorT1*		
Order (n)	*S*	*C*	*S*	*C*	*S*	*C*	*S*
0PN	0.5590	0.8590	0.5595	0.8403	0.3848	0.1627	0.41
1PN	0.3022	0.3487	0.3025	0.3500	0.1519	0.1612	0.15
1.5PN	0.7866		0.7771		0.7044		0.69
2PN	0.9795		0.9640		0.5650		0.59
2.5PN	0.5736		0.5736		0.5962		0.59
3PN	0.9525		0.9505		0.9915		0.92
3.5PN	0.9522		0.9508		0.9914		0.92

Total (Useful) Cycles

$$\mathcal{N}_{\rm tot} \equiv \frac{1}{2\pi}(\varphi_{\rm lso} - \varphi_{\rm low}) = \int_{F_{\rm low}}^{F{\rm lso}} dF \frac{N(F)}{F} \,,$$

$$N(F) \equiv F^2/\dot{F}$$

$$\mathcal{N}_{\rm useful} \equiv \left(\int_{F_{\rm low}}^{F{\rm lso}} \frac{df}{f} w(f) N(f) \right) \left(\int_{F_{\rm low}}^{F{\rm lso}} \frac{df}{f} w(f) \right)^{-1} \,,$$

$$w(f) \equiv a^2(f)/h_n^2(f);$$

$$h_n^2(f) \equiv f S_n(f);$$

$$|H(f)| \simeq a(t_f)/[\dot{F}(t_f)]^{1/2}$$

Total (Useful) Cycles - Test Mass

Initial LIGO noise spectrum.
Low frequency cutoff of 40Hz.

	$(1M_\odot, 10M_\odot)$		$(1M_\odot, 50M_\odot)$		$(1M_\odot$
Order (n)	S	C	S	C	S
0PN	481 (92.3)	424 (74.6)	118 (110)	77.8 (64.4)	13.6
1PN	560 (117)	526 (102)	180 (186)	124 (104)	25.7
1.5PN	457 (81.7)	433 (71.8)	88.8 (76.3)	58.5 (38.2)	8.4
2PN	447 (77.7)	440 (74.0)	77.0 (61.8)	62.5 (41.5)	6.1
2.5PN	464 (84.5)	454 (79.6)	96.8 (85.5)	74.5 (50.5)	9.7
3PN	442 (74.7)	440 (73.3)	64.5 (45.2)	58.1 (35.5)	3.4
3.5PN	445 (76.1)	442 (74.5)	68.7 (49.7)	60.6 (36.8)	4.0
4PN	445 (75.8)	443 (75.2)	66.4 (45.1)	62.9 (39.0)	2.9
4.5PN	443 (75.1)	442 (74.5)	63.7 (42.0)	60.0 (35.6)	2.5
5PN	444 (75.3)	443 (75.0)	63.8 (40.9)	62.2 (37.8)	2.1
Exact	442 (74.1)		59.1 (34.3)		0.9

Anomalous Cases

- Anomalous cases can be understood in terms of comparison of $E'(v)/\mathcal{F}(v)$ of the approximant with that of the 'Exact' WF together with the best-sensitivity BW of the detector
- In these cases though complete approximant better in modelling late inspiral, standard approximant is better in modelling early inspiral
- Since binary spends mores cycles in early inspiral, overlaps heavily influenced by accuracy of early inspiral model
- Comparison of various anomalous Detector results can be qualitatively understood in these terms

Conclusion

- *Standard Adiabatic* approximation to the phasing of GWs from ICB based on PN expansions of conserved energy and GW flux truncated at the *same relative* PN order.
- In terms of the dynamics of the binary, standard treatment equivalent to neglecting certain conservative terms in the acceleration.
- New *complete adiabatic* approximant is proposed which, in spirit, corresponds to a complete treatment of the acceleration accurate up to the respective PN order.

Conclusion .. Contd

- Test-mass: Effectualness of the templates improves significantly in the complete adiabatic approximation at lower ($<$ 3PN) PN orders.
- However, Standard adiabatic approximants of order $\geq$ 3PN are nearly as good as the complete approximants.
- Faithfulness of complete adiabatic approximants is generally better at all PN orders.
- There are some cases of anomalous behavior. In these cases early inspiral is better modelled by the standard approximants than the corresponding complete approximants

Conclusion .. Contd

- Complete adiabatic approximants are far superior to the standard adiabatic approximants in modelling the final inspiral.
- Complete adiabatic approximants generally less 'biased' in estimating the parameters of the binary.

Conclusion .. Contd

- Comparable-mass: Standard adiabatic approximants of order $\geq$ 1.5PN provide a good lower-bound to the complete adiabatic approximants for the construction of both effectual and faithful templates.
- Comparable-mass: Standard adiabatic approximants of order 2PN/3PN produce the target value 0.965 in effectualness (corresponding to 10% event-loss) in the case of the BH-BH/NS-NS binaries.
- Only the inspiral phase of the binary is considered. Plunge and quasi-normal ring down phases are neglected